

A GEOMETRIC FORMULATION OF FIDUCIAL PROBABILITY

Paul Gunther *

Abstract

The geometric formulation of fiducial probability employed in this paper is an improvement over the usual pivotal quantity formulation. For a single parameter and single observation, the new formulation is based on the geometric properties of an ordinary two variable function and its surface representation.

The following theorem is proved: A fiducial distribution for the continuous parameter θ exists if and only if (i) the continuous random probability distributions of x for different θ 's are non-intersecting, and (ii) the random distributions are complete, i.e. at the extreme values of θ the limiting probability distributions are zero and one for all x .

The proof yields also a complete characterization of random distributions that lead to fiducial distributions.

The paper also treats intersecting distributions and non-intersecting incomplete distributions. The latter, which are frequently encountered in a null hypothesis, are shown to be associated with intersecting “composite” distributions.

An appendix compares the pivotal and geometric formulations.

Introduction

Fiducial probability was introduced by Fisher in 1930 [2]. Since the 1960's, however, interest and research in the subject has practically ceased and fiducial probability for the most part rejected. (An exception is the recent paper by Hannig [5] on “generalized fiducial inference”.)

The approach adopted by Fisher, and generally accepted by researchers, can be characterized as a *pivotal quantity* (PQ) formulation. The present paper presents an alternative geometric formulation for fiducial probability that is based on the properties of any function of two variables and its surface representation.

*4515 38th Street NW, Washington, DC 20016, e-mail: {igunther@rcn.com}

Appendix A, which compares the PQ and geometric formulations, also identifies flaws in the PQ formulation. To better understand the problem it will be useful to briefly summarize the analysis as well as the considerations that led to the PQ formulation.

Early on it was seen by Fisher that for translation-scale parameters a pivoting quantity yielded both a random distribution and a fiducial distribution. Apparently the PQ was viewed as a necessary ingredient for obtaining a fiducial distribution. Fisher also presented this result in the form of a general equation relating fiducial and random distributions, that was applicable to all parameters. The equation, which actually defines what we call the geometric formulation, reflects the fact that the PQ formulation for translation-scale parameters is also a geometric formulation. The PQ property was apparently so convincing, however, that there was no need to pursue any alternative formulation.

A natural *pivoting extension* that provides a generalization to all parameters was obtained by defining a general PQ by the equation $F(x, \theta) = \text{constant}$. Pivoting consisted of inverting a monotone random probability function to obtain an equivalent confidence limit function. Careful scrutiny of this procedure in Appendix A shows, however, that this generalization is neither pivoting nor an extension.

The flaw in the PQ formulation may very well have contributed to the subsequent decline of fiducial probability research.

The benefits of the geometric formulation replacement are demonstrated by its achievements, such as the non-intersection condition for existence of fiducial distributions. Also obtained is the solution for the fiducial distribution and associated confidence limits for multiple observations (the derivation presented in Appendix A) that is applicable to all parameters. This problem was previously unsolved, ostensibly because it requires a (geometric formulated) fiducial argument rather than the random probability argument that sufficed for a single observation. This result also demonstrates the necessity for including fiducial theory as an integral part of parametric probability

theory.

The new geometric formulation may well lead to renewed interest and research into fiducial probability, especially in areas of multiple parameters and discrete parameters.

Except for Appendix A, the paper is devoted entirely to a non-intersection existence theorem and its consequences. Section 1 illustrates the determination of the fiducial distribution using the geometric formulation. Section 2 gives an example of intersecting distributions that is useful for the existence proof in Section 3. The proof includes a detailed analysis of “touching” distributions, and leads also to a complete characterization of non-intersecting configurations. Section 4 discusses the three dimensional fiducial surface and associated geometry that underlies the geometric formulation. Section 5 analyzes intersecting “composite” distributions, and its evolution into the exceptional case of non-intersecting incomplete fiducial distributions, which arise in many null hypotheses.

1 Geometric formulation of the fiducial distribution

This section uses a plane representation of the two variable function that forms the basis of the geometric formulation. (Section 4 provides a three dimensional surface representation.)

Definition CFM A *continuous fiducial model* for the single observation x and the single parameter θ satisfies the following three conditions:

- (a) the domains of x and θ are (finite or infinite) intervals;
- (b) x has a continuous probability distribution for each θ ;
- (c) for each x the probabilities in (b) are continuous functions of θ .

[We note that this definition includes sufficient statistics, which are well known to be treatable as a single observation.]

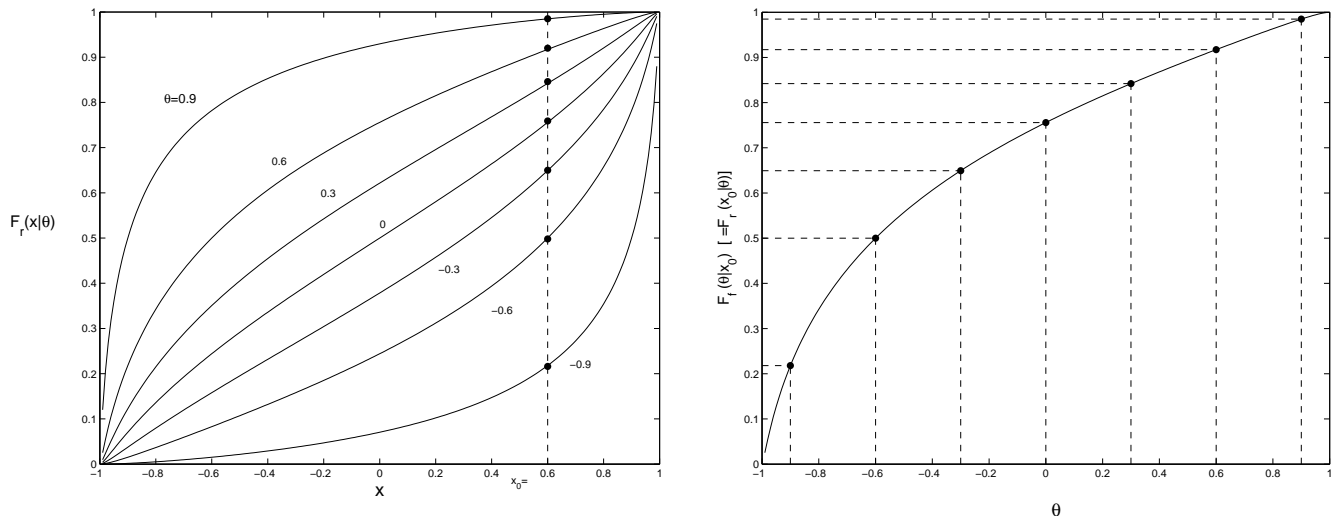


Figure 1: FD $F_f(\theta|x_0)$ derived from RD $F_r(x|\theta)$

Figure 1 illustrates application of the geometric formulation to determining the fiducial distribution (FD), $F_f(\theta|x)$, when the random distributions (RD), $F_r(x|\theta)$, are non-intersecting. For each fixed value of $x(=x_0$ say), the vertical line intersects the RD's for each θ at a probability value $F_r \equiv F_r(x_0|\theta)$, giving the points (F_r, θ) . Non-intersection of the RD's implies, as proven later (Theorem 1 in Subsection 3.2), that the F_r value varies monotonically with θ . The (F_r, θ) pairs, when plotted as $F_f(\equiv F_r)$ vs. θ (as shown in the right part of Figure 1) then constitute the fiducial distribution, $F_f(\theta|x_0)$, provided that the RD's satisfy also the following *completeness condition*: At the extreme values of θ the limiting RD's are identically zero and one, respectively, for all x (Theorem 2 in Subsection 3.2).

This construction motivates the following definition, which is justified by the theorems in Section 3 cited above.

Definition CFD *The (continuous) fiducial distribution for each x , $F_f(\theta|x)$, is the distribution induced on θ by the random probability distributions (RD), $F_r(x|\theta)$, when (i) the RD's for different θ 's are non-intersecting, and (ii) the RD's are complete, i.e. approach zero and one, respectively, for all x as θ approaches its two extreme values.*

The continuous fiducial model then becomes an *FD model*; otherwise, if either condition (i) or (ii) is not satisfied, we have a *non-FD model*.

Lindley's analysis in [7] of bayesian and fiducial distributions assumes condition (ii) and the monotone conclusion of (i).

The above construction, which defines the FD $F_f(\theta|x_0)$ as equivalent to the pairs, $(F_r(x_0), \theta)$, also describes a *geometric identity*. For the situation in Figure 1 where F_r is monotone increasing with θ (also referred to as θ increasing), the equation for this identity is

$$F_f(\theta|x_0) = F_r(x_0|\theta) \quad (F_r \text{ increasing with } \theta). \quad (1)$$

(In practice, this geometric identity is essentially equivalent to the geometric formulation.) At the minimum (infimum) value θ_m and maximum (supremum) value θ_M the completeness condition is: For all x ,

$$\lim_{\theta \rightarrow \theta_m} F_r(x|\theta) = 0, \quad \lim_{\theta \rightarrow \theta_M} F_r(x|\theta) = 1.$$

In almost all applications, however, F_r is monotone decreasing with θ . (x_0 then becomes the approximate median of the FD, as in the usual representation of translation parameters.) Replacing F_f by $1 - F_f$ yields

$$F_f(\theta|x_0) = 1 - F_r(x_0|\theta) \quad (F_r \text{ decreasing with } \theta). \quad (2)$$

(A corresponding change also occurs in the above completeness equations.) The density form of Eq. (2) is also Fisher's equivalence equation [3, p.70]. (Fisher apparently did not consider using it to replace the PQ formulation.)

Equations (1) and (2) are equivalent in the sense that replacing θ by $-\theta$ (or by $1/\theta$ when the θ domain is positive) converts either equation to the other. The symmetric Eq.(1) yields simpler analyses and is used throughout this paper, except for the example in Section 2.

The identity Eq.(2) can be expressed in terms of fiducial probability $P_f()$ and random probability $\text{Pr}()$. With X and Θ having the customary meaning associated

with random variables, we have:

$$Pr(X \geq x_0|\theta) = P_f(\Theta \leq \theta|x_0). \quad (3)$$

[The term “likelihood”, a common synonym for fiducial probability, probably represents the most appropriate interpretation to be associated with fiducial probability.]

Non-monotone measure for intersecting RD’s

The previous procedure for non-intersecting RD’s in Figure 1 yielded the points (F_r, θ) that comprised a monotone function. This function can also be viewed as an ordinary monotone measure. The relation is similar to that when the RD’s are complete: The monotone function becomes a fiducial distribution $F_f(\theta|x_0)$ which then defines a probability measure of sets from generalizations of the right side of Eq.(3).

The same procedure is applicable to intersecting RD’s. The points (F_r, θ) then comprise a non-monotone function, denoted by $m_f(\theta|x_0)$, which represents also an associated *non-monotone measure*. This is also referred to as a signed measure, being positive (say) when m_f is increasing and negative when decreasing. (A detailed treatment of signed measures is given in Halmos [4, Chapter 6].)

In addition, the fiducial distribution notation, $F_f(\theta|x_0)$, in the geometric identity Eq.(1) is replaced by $m_f()$ giving a *non-monotone geometric identity*:

$$m_f(\theta|x_0) = F_r(x_0|\theta).$$

We also employ the notation $M_f()$ to denote either a monotone or a non-monotone function, and with an associated *general fiducial measure (FM)* that can be either a monotone measure (when RD’s are non-intersecting) or a non-monotone measure (when RD’s are intersecting). (M_f is especially appropriate in the Section 3 proof prior to demonstrating existence of the positive measure FD.) The *generalized geometric identity* then becomes:

$$M_f(\theta|x_0) = F_r(x_0|\theta). \quad (4)$$

The same (F_r, θ) procedure also yields the following simple, but important, proposition:

Proposition FM

For any family of parametric RD's, both the general fiducial measure $M_f(\theta|x_0)$ and the generalized geometric identity Eq.(4) always exist.

A formal proof in terms of the surface $F(x, \theta)$ is given in Section 4. In brief, existence of M_f follows from the fact – applicable to any function $f(x, y)$ of two variables – that the functions of one variable, say $f(x|y)$, determine the related surface, which then also determines the functions of the other variable, $f(y|x)$. The relationship between the two functions is the geometric identity. When the values of $f(x|y)$ are RD probabilities one gets measure terminology.

We note that item (c) in the continuous fiducial model Definition CFM can now be restated as: (c') $M_f(\theta|x)$ is continuous for each x . The monotone FM conclusion of Theorem 1 in Section 3 requires only this continuity condition and the general geometric identity Eq.(4). We observe also that Definition CFD becomes the statement: The general fiducial measure $M_f(\theta|x_0)$ becomes a fiducial probability distribution $F_f(\theta|x_0)$ iff the RD's satisfy conditions (i) and (ii).

2 Non-FD joined distribution

In connection with the proofs in Section 3, it is useful to first consider a non-FD example. A simple such example can be obtained by joining two different RD types. Assuming an unknown (decreasing) translation parameter θ , a normal distribution for $\theta > 0$ could be joined to (say) a Cauchy distribution for $\theta < 0$, or more simply to merely another normal distribution with a different known standard deviation. For computational ease we join two families of uniform distributions with different semi-ranges (equal to one-half the range) (see Figure 2(a)). Continuity can be achieved by introducing a θ transition interval, $[-\theta_T, +\theta_T]$, with transition RD's that vary mono-

tonically with θ from the RD at $+\theta_T$ to the RD at $-\theta_T$. (Otherwise, as shown below, one gets a discontinuity at $\theta = 0$.) The semirange is b for $\theta < -\theta_T$ and a ($a < b$) for $\theta > \theta_T$.

We assume a linear variation of the semiranges in the transition interval, $-\theta_T < \theta < +\theta_T$, yielding the semiranges $T(\theta)$:

$$T(\theta) = b[1 - \theta/\theta_T]/2 + a[1 + \theta/\theta_T]/2. \quad (5)$$

The RD cumulative probability corresponding to a semirange S , which is a , b or $T(\theta)$ depending on the appropriate θ interval, is:

$$F_r(x|\theta) = \frac{1}{2} + \frac{x - \theta}{2S}, \quad -S \leq x - \theta \leq S.$$

We note that all θ RD's in the transition interval pass through the point x_T where the a and b RD's for $\pm\theta_T$, respectively, intersect (see Figure 2(a)). We have

$$x_T = \frac{b + a}{b - a}\theta_T,$$

with corresponding probability

$$F_T \equiv F_r(x_T|\pm\theta_T) = \frac{1}{2} + \frac{\theta_T}{b - a}.$$

(x_T, F_T) is also the vertex of a conical *intersection region* with sides formed by these same a and b RD's.

Figure 2(a) plots the RD's for numerical values $a = 1$, $b = 4$, $\theta_T = .5$, yielding the transition intersection point $x_T = 5/6$ with probability $F_T = 2/3$. The RD intersection region is defined by $x > (5/6)$ and $\theta \in [-.5, +.5]$. At each point (x, F_r) in this region, three different RD's intersect, corresponding to semirange a , semirange b and transition semirange $T(\theta)$.

The intersections are shown more clearly in Figure 2(b), which plots the (signed) fiducial measure for $x = 1.25$ ($> x_T$) and $x = .5$ ($< x_T$). The ordinate is $1 - m_f(\theta|x)$ rather than $m_f(\theta|x)$ in order to show more directly the relationship with the RD's in Figure 2(a); since θ is a decreasing parameter, it is now $1 - m_f(\theta|x)$ that equals F_r . The

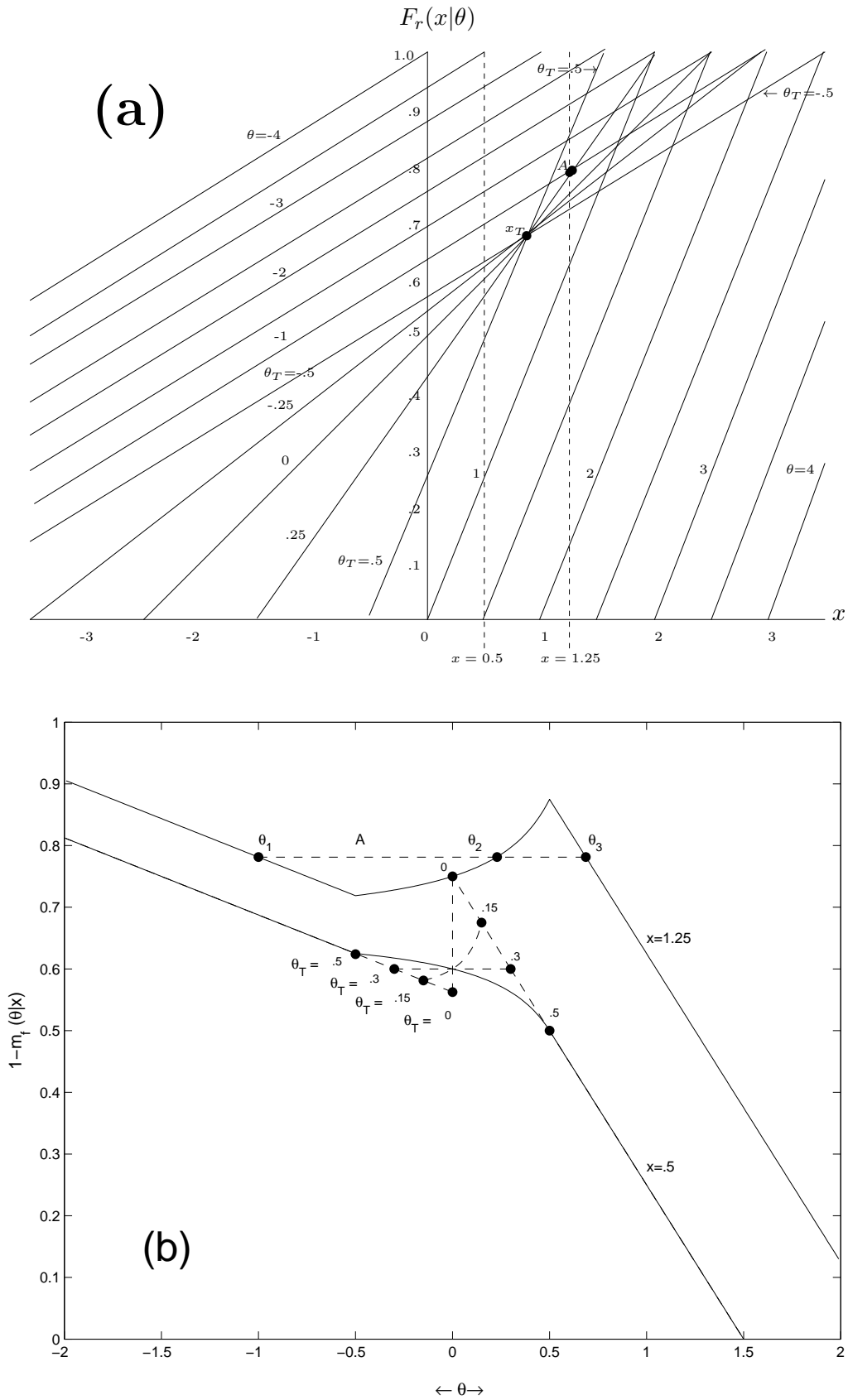


Figure 2: (a) Non-FD joint distributions, (b) non-monotone FM for intersecting RD's

fiducial curve for $x = 1.25$ consists of three parts: The monotone decreasing linear part on the left corresponds in Figure 2(a) to the values of F_r as one proceeds downward on the $x = 1.25$ vertical line with semirange b RD's from $\theta = -2.75$ to $\theta = -.5(= -\theta_T)$, the lower boundary of the intersection region. For the second intermediate part, one has a monotone increasing transition curve with variable transition semiranges from $\theta = -\theta_T$ to $+\theta_T$; these correspond in Figure 2(a) to the F_r values as one proceeds upward from the lower ($-\theta_T$) to the upper ($+\theta_T$) transition boundary. The third monotone decreasing linear part, similar to the first part, corresponds in Figure 2(a) to the values of F_r as one proceeds downward with semirange a RD's from $\theta = .5(= +\theta_T)$, the upper boundary of the intersection region, to $\theta = 2.25$.

In Figure 2(a) the point (labeled A) at $x = 1.25$ and $F_r = 0.78$, corresponds on the Figure 2(b) $x = 1.25$ curve to fiducial measure $1 - m_f = 0.78$ (the horizontal line A), and yields the three intersections: $\theta_1 = -1$ for the RD with semirange $b = 4$; $\theta_2 = .25$ for the transition RD with semirange $T(.25) = 1.75$; and $\theta_3 = .68$ for the RD with semirange $a = 1$.

The $1 - m_f$ fiducial curve for $x = .5$, being less than the intersection $x_T = .83$, is monotone decreasing for all θ . Also shown (by dashed lines) is the effect of reducing the transition interval $[-\theta_T, +\theta_T]$. When $\theta_T = .3$ the intersection point $x_T = .5$ is the same value used to obtain the $x = .5$ fiducial curve. Hence the fiducial transition is constant, reflecting the fact that the vertical line in Figure 2(a) passes through x_T . Further reduction to the $\theta_T = .15$ curve places the $x = .5$ line of Figure 2(a) in the intersection region with an increasing fiducial transition curve. As θ_T and x_T approach zero the fiducial transition degenerates into a discontinuous vertical jump. The final paragraphs below discuss further the discontinuous solution.

We emphasize several features of this example. Depending on the value of x , there exist both non-intersecting RD regions where the fiducial measure $m_f(\theta|x)$ is monotone and hence constitutes a formal distribution, and also intersection regions where m_f is non-monotone and hence not a distribution. (The non-FD label affirms that a fiducial

distribution analysis is meaningful only if applicable to all admissible observations.) Another feature is the existence, for values of x where intersections occur, of multiple values of θ having the same fiducial measure $m_f(\theta|x)$. This is characteristic of a non-monotone measure, and is in fact a necessary and sufficient condition for non-monotonicity (Theorem EQ/NM in Appendix B).

The discontinuous solution

The transition interval has degenerated to a point $\theta_T = 0$ and hence contains no RD. However, the intersection region still exists, bounded by the semirange a and b RD's and by $x > 0$. In this region each value of m_f still yields three intersections, corresponding to semirange a and b RD's plus the intersection with the vertical jump. Although this last intersection is not associated with any RD, one can obtain a *normalized transition RD** corresponding to the normalized parameter $\theta^* \equiv \theta/\theta_T$, ($-1 \leq \theta^* \leq +1$). In fact, the previous Eq.(5) for semirange $T(\theta)$ can be interpreted as a formula for a normalized semirange $T^*(\theta^*)$ and corresponding normalized RD*. Together they constitute a *transition protocol* that is applicable to all θ_T . The actual non-normalized transition RD's and associated θ 's for a specific non-zero θ_T are obtained from $\theta = \theta^* \cdot \theta_T$. In the limit the normalized θ^* 's apply also to $\theta_T = 0$, and a normalized RD* can then be associated with the m_f intersection on the vertical discontinuity.

This RD* solution for $\theta_T = 0$ can be viewed in either a negative or a positive light. For the former the RD* value obtained depends upon an assumed transition protocol, although the discontinuous formulation with joining at $\theta = 0$ does not involve any transition. Consequently RD* is essentially indeterminate. The opposing positive view is that associating the $\theta = 0$ discontinuity with the limit of *any* transition protocol illuminates the underlying nature of the discontinuity. It is not really necessary to assign a specific RD* value.

3 Fiducial non-intersection theorems

This section proves necessary and sufficient conditions for an FD to exist. These are implied assumptions in almost all applications.

Theorem 1 *The fiducial measures (FM) $M_f(\theta|x)$ are monotone for each x iff the RD's $F_r(x|\theta)$ are non-intersecting for all θ .*

(For brevity we often write $M(\theta) \equiv M_f(\theta|x)$.)

3.1 Strict non-intersection

We consider first the simpler case of *strictly non-intersecting* RD's, i.e. completely separated with different θ RD's having no points in common, together with corresponding *strictly monotone* FM's, i.e. no intervals where FM is constant. (The complete non-strict case is treated below in Theorem 1.)

Strict non-intersection does not apply to finite endpoints x_m and x_M where the same probability, $F_r = 0$ or 1 , applies to all RD's and the corresponding FM $M_f(\theta|x_{m/M})$ is constant. More generally, this *endpoint condition* exists when an intersection point is common to all θ .

Theorem 1S *$M_f(\theta|x)$ is strictly monotone for each x iff the RD's $F_r(x|\theta)$ for different θ are strictly non-intersecting.*

We recall, and cite for reference, the following well known definition: *$M(\theta)$ is a strictly monotone increasing (say) function iff for all $\theta_2 > \theta_1$ we have $M(\theta_2) > M(\theta_1)$.*

This definition is of course a special case of the general monotone definition wherein the above $>$ relation is replaced by \geq , giving $M(\theta_2) \geq M(\theta_1)$. Note that these definitions allow discontinuous jumps. It is more convenient, however, to introduce continuity when applying Lemma 1 below.

The lemma is a generalization of the intermediate value property of a continuous function. For example, for any non-monotone function we have: if points 1 and 3 are

on opposite sides and in a neighborhood of a (point 2) maximum (say), then one can draw a horizontal line between point 2 and points 1, 3.

Lemma 1 *Let $f(z)$ be a continuous function. Suppose the ordered points $z_1 < z_2 < z_3$ have corresponding values of $f(z_i)$ that are not in monotone order, i.e. $f(z_1) < f(z_2) > f(z_3)$ or $f(z_1) > f(z_2) < f(z_3)$. Then there exist points z_1^*, z_2^* such that $f(z_1^*) = f(z_2^*)$.*

Proof: For the case $f(z_1) < f(z_2) > f(z_3)$ let f^* be such that $f(z_2) > f^* > \max\{f(z_1), f(z_3)\}$. For the continuous segment (z_1, z_2) the intermediate value theorem for a continuous function yields z_1^* such that $f(z_1^*) = f^*$. Likewise, for the continuous segment (z_2, z_3) there exists $z_2^* (> z_1^*)$ such that $f(z_2^*) = f^*$. The proof for the other non-monotone case is similar. ■

For later application we use the following simple extension of Lemma 1:

Corollary *In addition to the assumptions of the lemma, let M_1, M_2, \dots be any finite or denumerable set of numbers. Then z_1^*, z_2^* exist such that both $f(z_1^*) = f(z_2^*)$, and which are also not equal to M_i ($i = 1, 2, \dots$).*

Proof: The set of admissible function values f^* in the proof of the lemma includes an open set \mathcal{F} , say. The difference subset $\mathcal{F} \setminus \{M_1, M_2, \dots\}$ subtracts at most a denumerable set from \mathcal{F} whence the remainder is non-empty. ■

Proof of Theorem 1S: Suppose that the continuous RD's $F_r(x|\theta)$ are strictly non-intersecting. We initially presume, until monotonicity of the FM with respect to θ is proven, that a θ numerical value (in the interval domain specified as assumption (a) in the Section 1 fiducial model Definition CFD) is attached to each different RD and constitutes an arbitrary “label” for the RD. Then for each x and all $\theta_i \neq \theta_j$, strict non-intersection implies that $F_r(x|\theta_i) \neq F_r(x|\theta_j)$. Equivalently, in terms of the FM we have, from the geometric identity Eq.(4), that $M(\theta_i) \neq M(\theta_j)$. We need to prove that continuity of $M(\theta)$ implies that $M(\theta)$ is strictly monotone.

Let θ' and $\theta'' (> \theta')$ be an arbitrary “reference” pair and suppose that $M(\theta'') >$

$M(\theta')$. (The opposite case, $M(\theta'') < M(\theta')$, is treated similarly.) For any θ_1, θ_2 pair with $\theta_2 > \theta_1$ (not necessarily different from θ' or θ'') we will show that continuity of $M(\theta)$ implies that $M(\theta_2) > M(\theta_1)$. Suppose the contrary, that $M(\theta_2) < M(\theta_1)$, and consider the six different inequality cases satisfied by the four θ 's, in combination with the various corresponding relative positions (inequalities) of the four quadruplet values, $M(\theta_1), M(\theta_2), M(\theta'), M(\theta'')$ (abbreviated to M_1, M_2, M', M''), that satisfy the two assumed inequalities. It is readily seen that at most three of the four M 's can be monotonically related; moreover, an appropriate selection of two M 's from any such monotone triplet, together with the fourth M , will comprise a non-monotone M triplet.

For example, consider the case $\theta' < \theta_1 < \theta_2 < \theta''$. If $M_1 < M'$, then the triplet $M' > M_1 > M_2$ is monotone decreasing and selecting any two of these together with M'' , is a non-monotone triplet. (If $\theta_1 = \theta'$ the resultant triplet is already non-monotone.) For the case where $M_1 > M''$ and $M_2 < M'$, all triplets are non-monotone.

Thus the requirements of Lemma 1 are satisfied, and there exist $\theta_1^* \neq \theta_2^*$ with $M(\theta_1^*) = M(\theta_2^*)$, which contradicts the non-intersection condition that $M(\theta_1^*) \neq M(\theta_2^*)$. Hence $M(\theta_2) > M(\theta_1)$ and $M(\theta)$ is strictly monotone increasing. Similarly, if initially $M(\theta'') < M(\theta')$, then $M(\theta)$ is strictly monotone decreasing.

For the converse, $M_f(\theta|x)$ is assumed for each x to be either strictly monotone increasing or decreasing. If the former, then for all x , $\theta_2 > \theta_1$ implies that $M(\theta_2) > M(\theta_1)$. That is, the RD's at each x , $F_r(x|\theta)$, are separated for different θ 's. Combining these $F_r(x|\theta)$'s for varying x yields separated and hence strictly non-intersecting RD's. Similarly for monotone decreasing. ■

The four θ 's and inequalities in the proof are also the same as in Definition NM in Appendix B of an (assumed contrary) non-monotone $M(\theta)$. We also remark that a variation of the proof merely cites the non-monotone Theorem EQ/NM, also in Appendix B, wherein a continuous non-monotone $M(\theta)$ implies existence of $M(\theta_1) = M(\theta_2)$, and thereby providing the contradiction needed to prove Theorem 1S. However,

the proof of Theorem EQ/NM is essentially the same as for Theorem 1S and also requires the use of Lemma 1.

We note also that the assumption of FM continuity (item (c) or (c') in Definition CFM) can be relaxed to permit a denumerable number of jumps. This would be applicable, however, only for RD's with both a continuous and a discrete component.

3.2 General non-intersection

Touching

Different RD's may be non-intersecting even though they have points in common. This occurs when RD's *touch* at a point x_0 , say. For two RD's with $\theta_1 < \theta_2$ we have: (i) $F_r(x_0|\theta_1) = F_r(x_0|\theta_2)$, and (ii) for right and left (non-touching) neighborhoods of x_0 , with elements denoted by $x+$ and $x-$, respectively, the monotone directions with θ are the same, i.e. for monotone increasing (say) with θ , we have both $F_r(x+|\theta_1) < F_r(x+|\theta_2)$ and $F_r(x-|\theta_1) < F_r(x-|\theta_2)$.

(When RD derivatives exist, the RD's are tangent and unequal convexities (say) yield (ii).) (An intersection satisfies condition (i), but in (ii) the monotone directions in right and left neighborhoods are opposite.)

Touching at x_0 necessarily includes all intermediate θ in the closed interval $[\theta_1, \theta_2]$. The corresponding RD's are also, because of continuity, intermediate to the θ_1 and θ_2 RD's in the right and left neighborhood inequalities, and hence necessarily pass through x_0 . (A formal proof is included in the proof below of Theorem 1.) (A different route is taken by intersecting RD's in reaching the reverse inequality in (ii); see the Section 2 example.)

$[\theta_1, \theta_2]$ is a maximum size interval (assumed hereafter) iff all θ that are either $< \theta_1$ or $> \theta_2$ are non-touching in the neighborhoods of x_0 . $M_f(\theta|x_0)$ is constant for $\theta \in [\theta_1, \theta_2]$. Indeed, existence of touching intervals is necessary and sufficient for a FM to be non-strict, and also for non-intersecting RD's to be non-strict.

For the same x_0 , $M_f(\theta|x_0)$ may contain several touching intervals. The θ intervals

are disjoint since the F_r values are different. Between two successive constant FM intervals is an open interval of non-touching θ 's with strictly monotone $M_f(\theta|x_0)$.

Additional touching properties are presented following the proof of Theorem 2.

Proof of Theorem 1

We first restate the usual definition of general monotonicity to allow explicitly for constant intervals, by separating the \geq relation into $=$ and $>$.

Definition GM $M(\theta)$ is monotone increasing (say) iff: (i) $M(\theta) = M_i, (i = 1, \dots)$ for θ in disjoint intervals I_i ; otherwise (ii) for any pair (θ_1, θ_2) not in the same I_i (the set of such pairs is denoted by \mathcal{P}), we have that $\theta_2 > \theta_1$ implies $M(\theta_2) > M(\theta_1)$.

As before, jumps are not precluded, in either (i) or (ii), but are later eliminated when continuity of $M(\theta)$ is introduced.

It is convenient to relate (using notation (i') and (ii')) each part of the proof to each part ((i) and (ii)), respectively, in the above Definition GM. The non-intersection RD's $F_r(x|\theta)$, with arbitrary θ labeling (as in the proof of Theorem 1S), have for each x , θ 's that are either: (i') within disjoint touching sets $E_i (i = 1, \dots, n_x)$, or are (ii') non-touching. The non-intersection condition implies: (i') for the touching sets E_i we have $M(\theta) = M_i$ for all θ in E_i ; and (ii') for all pairs θ_1, θ_2 in \mathcal{P} , we have that $\theta_2 \neq \theta_1$ implies $M(\theta_2) \neq M(\theta_1)$.

Re (i'): We need to show that continuity of $M(\theta)$ implies that E_1 (say) is an interval I_1 . If, to the contrary, E_1 were not an interval, there would exist one or more gaps. That is, there exist $\hat{\theta}$ not in E_1 and a pair (θ_1, θ_2) in E_1 such that $\theta_1 < \hat{\theta} < \theta_2$. Now $M(\hat{\theta})(\equiv \hat{M}) \neq M_1$, say $> M_1$ (the other $<$ case is similar), whence $M_1 = M(\theta_1) < M(\hat{\theta}) > M(\theta_2) = M_1$. Since $M(\theta)$ is continuous, it follows from the Corollary to Lemma 1 that for M'^* satisfying both $M_1 < M'^* < \hat{M}$ and also $M'^* \neq M_i, (i = 2, \dots)$, there will exist θ'_1 and θ'_2 with $M(\theta'_1) = M(\theta'_2) = M'^*$. Since the pair (θ'_1, θ'_2) is in \mathcal{P} this contradicts the non-intersection assumption that $M(\theta'_1) \neq M(\theta'_2)$ for all θ pairs in \mathcal{P} . Hence $\hat{\theta}$ is in E_1 , there is no gap, and E_1 is an interval I_1 . Similarly, for

$M(\hat{\theta}) < M_1$ and for $i > 1$. Hence (i') becomes (i).

Re (ii'): The proof is practically the same as in Theorem 1S. Let θ' and $\theta''(> \theta')$ be a reference pair in \mathcal{P} with (say) $M(\theta') < M(\theta'')$, and let θ_1 and $\theta_2(> \theta_1)$ be any pair in \mathcal{P} . Suppose, contrariwise, that $M(\theta_1) > M(\theta_2)$. For any relative position of the four θ 's and corresponding $M(\theta)$'s, then, as in the proof of Theorem 1S, there always exists a non-monotone $M(\theta)$ triplet. The Corollary to Lemma 1 then yields two θ^{*} 's in \mathcal{P} with equal $M(\theta^{*})$'s. Hence a contradiction and $M(\theta_1) > M(\theta_2)$ in \mathcal{P} . Similarly for decreasing monotonicity, $M(\theta') > M(\theta'')$. Hence $M(\theta)$ is monotone in \mathcal{P} , (i.e., for non-touching θ 's) and (ii') becomes (ii). Hence $M_f(\theta|x)$ is monotone for all x .

Conversely, let $M_f(\theta|x_0)$ be monotone increasing (say) for each x_0 . (a) When $M_f(\theta|x_0) = \text{constant}$ for disjoint intervals $[\theta_{1j}(x_0), \theta_{2j}(x_0)]$, ($j = 1, \dots, m_j(x_0)$), then equivalently the RD's $F_r(x_0|\theta)$ are touching for θ 's in these touching intervals. (b) When M_f is strictly increasing in an interval, the equivalent $F_r(x_0|\theta)$ is also strictly increasing with θ . Combining both (a) and (b) F_r 's for all x 's (replacing the x_0 notation) yields a non-intersecting configuration. Similarly for M_f monotone decreasing, which proves the converse. ■

There exists also an *endpoint solution* – discussed in the intersection analysis in Appendix B – corresponding to an endpoint condition where all RD's intersect at the same point $x_I \neq 0, 1$, and thereby constituting a common endpoint for two adjacent FM's. (An example is a scale parameter for an asymmetrical distribution having both positive and negative values.) Although such a solution formally satisfies the monotone conditions for Theorem 1, it is not applicable to the (implicit) single fiducial model and can be disregarded.

We note the following symmetric relation between F_r and M_f :
 $M_f(\theta|x)$ is [strictly] monotone for each x iff $F_r(x|\theta)$ is [strictly] non-intersecting for different θ 's. Contrapositively, $F_r(x|\theta)$ is [strictly] monotone for each θ iff $M_f(\theta|x)$ is [strictly] non-intersecting for each x .

Similar relations exist regarding touching and constant intervals; and also com-

pleteness (in Theorem 2 below).

FD existence theorem

Theorem 2 *A FD exists iff the RD's are non-intersecting and complete.*

Proof: From Theorem 1, RD's are non-intersecting iff the FM's are monotone for all x . Also, by definition, monotone FM's are (fiducial) distributions iff the extreme values of $M_f(\theta|x)$ are 0 for θ_m (say) and 1 for θ_M , for all x , i.e. the RD's are complete. (More accurately, for increasing (say) θ , $\lim_{\theta \rightarrow \theta_m} F_r(x|\theta)(= M_f(\theta|x)) = 0$ for all x , and similarly $= 1$ for θ_M . These limiting distributions are discontinuous at finite endpoints x_M and x_m .) ■

Note that the endpoint solution does not satisfy the 0,1 limits.

Ordinarily, if non-intersecting RD's are incomplete, completeness can be achieved by supplementing with additional non-intersecting RD's; the RD's can then be said to be *completable*. An important exception is the incompletable non-central chi-square distribution. (See Subsection 5.2) In contrast to the non-intersection condition, completeness is a boundary-type condition. It is indicated in Subsection 5.2 that incompletable distributions occur only for certain non-FD “composite” distributions.

Touching segments

In addition to a touching θ interval at x_0 , suppose there is also touching at $x'_0 (> x_0)$. This can occur following an open right non-touching neighborhood about x_0 , which serves also as a left neighborhood about x'_0 for the new touching θ 's.

Such touching can be continuously extended to an entire x -interval, say $[x_1, X]$. The θ interval need not be the same for all x in $[x_1, X]$. Changes consist in adding or removing θ 's while incorporating transition neighborhoods similar to those in successive point touchings. The result is that changes can occur only at discrete points x_i ($i = 1, \dots, n$), with an open x -interval between changes serving as a transition. When adding θ 's at x_i the new touching θ interval also begins at x_i , but when removing θ 's the actual reverting to non-touching status takes effect at x_i+ , the “beginning” of the

open right neighborhood of the removed θ 's. [The notation x_i+ (which differs slightly from the previous usage) to denote a “beginning”, is merely suggestive. A rigorous condition states that θ is non-touching in all right (sufficiently small) ϵ neighborhoods of x_i .] When both addition and removal occur, only the added θ 's are included at x_i , while the touching θ 's that remain after the removals appear at x_i+ . Changes in θ 's can be to the beginning and/or the ending of the previous $[\theta_1, \theta_2]$ interval.

The beginning x_1 of an entire x -interval constitutes the initial addition change of RD's from non-touching to touching status, while $x_n(\equiv X)$ is the last touching before removal of all remaining RD's to non-touching status at x_n+ . Point touching at x_0 is the special degenerate interval case, $x_1 = x_n(= x_0)$, with θ touching starting at x_0 and removal at x_0+ .

The above changes have been viewed relative to increasing values of x . The same result is obtained if x decreases from x_n to x_1 ; previous additions are treated now as removals and previous removals treated as additions.

These results can be expressed as a *touching segment* that consists of a θ *touching interval function* $[\theta_L(x), \theta_U(x)]$ for x in the segment domain $[x_1, X]$. $\theta_L(x)$ and $\theta_U(x)$ are each step functions with jump discontinuities at discrete points $x_1, \dots, x_n(= X)$. At an x_i discontinuity $\theta_U(x_i)$ assumes the larger of the two values that are before and after the discontinuity. For adding θ 's this is the value after the positive jump; for removing θ 's it is before the negative jump. Both adding and removing (different) θ 's can be viewed as combining a positive jump at x_i followed (almost) simultaneously by a negative jump; this yields an isolated discontinuity at x_i with value $\theta_U(x_i)$ that corresponds to the positive jump.

Similarly for $\theta_L(x)$ with “smaller value” replacing “larger value” in the above.

Associated with an RD touching segment is a common non-decreasing RD section $F_T(x) \equiv F_r(x|\bar{\theta}(x))$ where for each $x \in [x_1, X]$, $\bar{\theta}(x) \equiv [\theta_L(x), \theta_U(x)]$.

An *RD non-intersection configuration* corresponds to the RD touchings that occur for a particular arrangement of N disjoint touching segments $\chi_j, (j = 1, \dots, N)$.

All such segment arrangements, together with $N = 0$ for strict (no touching) non-intersections and also $x_1 = X$ for point touchings, constitute a characterization of the entire class of RD non-intersecting configurations. [Not addressed is the possibility of a denumerable number of touching segments and denumerable changes within each segment; this might affect the completeness of the characterization.]

An *analysis of intersections* appears in Appendix B.

4 The $F(x, \theta)$ fiducial surface

A three dimensional version of Figure 1 with θ presented on a separate axis yields a surface $F(x, \theta)$ that represents the geometric formulation. The RD $F_r(x|\theta_0)$ for given θ_0 constitutes a *random θ section* of the surface, i.e., the RD is the intersection (curve) of the surface with the vertical plane $\theta = \theta_0$. The entire surface $F(x, \theta)$ is generated by all the θ sections. Similarly, each FM, $M_f(\theta|x_0)$, corresponds to a *fiducial x section*; all of these sections likewise generate the surface. The geometric formulation in Section 1 starts by specifying the RD θ sections, $F_r(x|\theta)$; these generate the surface $F(x, \theta)$ which in turn yields the fiducial x sections. In Proposition FM of Section 1 this proves existence of the FM $M_f(\theta|x_0)$.

To prove the geometric identity Eq.(4) we note that each individual point (x_0, θ_0) lies on both a θ_0 section and an x_0 section. Hence the fiducial measure $M_f(\theta_0|x_0)$ equals the random probability $F_r(x_0|\theta_0)$. Letting θ_0 vary (as θ) and with accompanying variable points (x_0, θ) , each fiducial x_0 section $M_f(\theta|x_0)$ is equal to the value at x_0 of each corresponding RD θ section, $F_r(x_0|\theta)$, thereby giving the geometric identity.

The two-dimensional *random plane* plot (as in Figure 1 and Figure 2(a)) of the RD's for different θ 's consists of projections of a finite number (to be visually meaningful) of θ sections onto the $F(= F_r) - x$ plane. They comprise superpositions of θ section RD's such as obtained when the surface is viewed from the θ axis direction. In the nomenclature of Subsection 3.2 this also constitutes the RD configuration. (The geometry of the configuration is the same whether or not the θ sections vary continuously

with θ .) Similarly the *fiducial plane* representations, as in Figure 2(b), are projections of x -sections onto the $F(= M_f) - \theta$ plane; equivalently, superimposed x -sections as viewed from the x axis direction. This constitutes an FM configuration that is dual to the RD configuration.

The plane representations provide a clearer picture of intersecting RD's and non-monotone m_f 's than does the surface representation. The latter, however, conveys more simply the continuity requirement, with the three (a)-(c) continuity conditions in the Section 1 definition of fiducial model being replaced simply by continuity of $F(x, \theta)$.

[Graves has proven in [4, Theorem 5, p.102] that for a surface $f(x, y)$ to be continuous at a point (x, y) requires that the continuity of a y section, $f(x|y)$ say, at that point be uniform in y . Graves gives an example showing that otherwise a discontinuity can result. It is not clear, however, whether uniformity in θ is needed for the monotone distribution functions.]

The fiducial surface geometry

For purpose of describing the $F(x, \theta)$ surface, suppose that the x and θ domains each consist of the unit interval $[0, 1]$. Together with the zero-one probability range for the ordinate F , the surface will then lie within the unit cube shown in Figure 3.

We further initially suppose the surface to be an inclined plane passing through the vertices 1278 in Figure 3; equivalently, through the base edge 12 and its diagonally opposite edge 78. Along these two edges the RD's have probabilities of zero and one, respectively. The RD random plane projection consists of a single 45 degree line applicable to all θ , while the fiducial plane projection consists of horizontal parallel lines. The RD's can be separated by pushing down side 27 toward the base edge 23, and simultaneously pulling side 18 upward toward top edge 58. When (approximate) coincidences with edges 23 and 58 are reached, the RD's become complete. If the stretchings of the inclined plane are "smooth" (no distortions, as explained below)

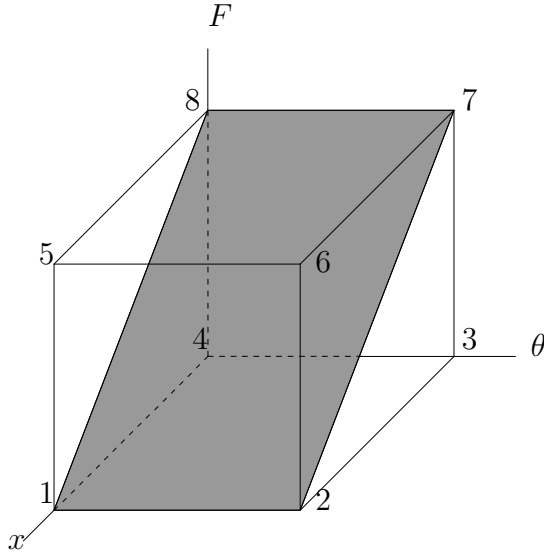


Figure 3: Inclined plane (1278) as preliminary $F(x, \theta)$ surface for FD

the monotone random plane RD projections will be non-intersecting. The result is a FD surface where the x section $M_f(= F_f)$ curves are monotone, non-intersecting and complete.

This FD surface is symmetric about the surface curve (with endpoints 2 and 8) that results from intersecting the surface with the vertical plane through vertical edges 26 and 48 – equivalently, through the diagonally opposite vertices 2 and 8. The surface proceeds “monotonically” from the base-anchored edges 12 and 23 to the top-anchored edges 58 and 87; vertices 2 and 8 become the symmetric vertex anchors. The symmetric-like aspect resides in the fact that interchanging the two surface portions on each side of the symmetric curve 28 (which is equivalent to interchanging RD and FD) retains the monotone character of the surface.

Opposite monotonicity of parameter θ is obtained by changing the directions of the θ and x axes. Other variations correspond to having symmetric base anchors at each of the four base vertices. We can state then the following characterization of FD’s: The surface for an FD model consists of a symmetric monotone surface that progresses from two adjacent base edges to diagonally opposite adjacent top edges.

A non-FD surface with intersecting RD's contains depressions, or bulges, that destroy the monotonicity. Consider, for example, the joined distributions in Section 2, F_1 and F_2 , with transition interval $\pm\theta_T$ (assuming, however, a finite domain). Until the transition is reached one has a monotone F_1 surface with section RD's $F_{r_1}(x|\theta)$ that are monotone increasing in the interval $[\theta_m, -\theta_T]$; the final RD is the $-\theta_T$ section $F_{r_1}(x|-\theta_T)$. After the transition there is likewise a monotone increasing F_2 surface for θ sections in the interval $[+\theta_T, \theta_M]$, starting with $F_{r_2}(x|+\theta_T)$. In the transition interval the surface sustains a depression region for $x > x_T$ because of the θ change to monotone decreasing (i.e. the x -partial derivative of F becomes negative) and continues until the terminal change at $+\theta_T$ reverts to monotone increasing. The planar RD's intersect in the depression region and the planar fiducial measures are non-monotone. For $x < x_T$ the surface is monotone increasing.

Reciprocal distributions

The fiducial surface $F(x, \theta)$ can be generalized to include non-monotone θ sections $m_r(x|\theta)$. In fact, a *reciprocal* m_r and F_f relation can be obtained by interchanging x and θ in the operations that lead, for example, to non-FD “composite” random variables, as discussed in the following Section 5. One obtains not only the dual FM which is equivalent to the RD distribution, but also, after an interchange, a valid reciprocal FM which is not equivalent to the RD's. Confusion between these two fiducials can occur, as noted in Subsection 5.2.

5 Composite distributions

Composite variables and their distributions are the simplest and most frequently occurring case of intersecting RD's. Moreover, their analysis sheds light on the nature of non-intersecting incomplete RD's, which is the exceptional non-FD case implied by Definition CFD in Section 1.

A simple example of a composite variable is $y \equiv |x|$: Each value of y is the composite

of $+x$ and $-x$; the distribution of y is then a composite distribution. More generally: $y \equiv g(x)$ is a **composite variable** iff $g(x)$ is not a continuous, strictly monotone function.

If $g(x)$ is not composite, i.e. is continuous and strictly monotone (equivalent to 1-1, which is the generalization for several variables), then the distribution of y is obtained from that of x in the usual manner as $F(g^{-1}(x))$.

We make the following conjecture:

For an FD model with RD's $F_r(x|\theta)$, let $g(x) \equiv y$ and/or $h(\theta) \equiv \phi$ be composite variables. Then the composite distributions of y and/or ϕ comprise a non-FD model.

We consider the following composite example, the analysis of which indicates that the above conjecture is almost certainly true. Let θ be an increasing translation parameter so that the RD and FD are given by: (For simplicity we use the same symbol F as in $F(x, \theta)$.)

$$F_r(x|\theta) = F(x + \theta) = F_f(\theta|x).$$

(More generally, with a translation parameter all subsequent definition formulas are readily shown to apply to both RD and FM.) We consider first the composite variable $g(x) = |x| \equiv y$, and later also $h(\theta) = |\theta| \equiv \phi$. We treat both the asymmetric *extreme value distribution (EVD)* (writing $F_{EVD}()$ as $F()$)

$$F(x + \theta) = 1 - e^{-e^{x+\theta}},$$

and also the symmetric normal distribution $N(x + \theta)$.

5.1 EVD composite I: Distribution of y

The RD of $y \equiv |x|$, denoted by $F_r^*(y|\theta)$, is obtained from the following well known probability relations:

$$\begin{aligned} \Pr(0 \leq Y \leq y) &= \Pr(X \in (0, y)) + \Pr(X \in (-y, 0)) & (6) \\ &= \Pr(-y \leq X \leq y) \\ &= \Pr(-\infty < X \leq y) - \Pr(-\infty < X \leq -y). \end{aligned}$$

Hence the composite RD and FM are

$$F_r^*(y|\theta) = F_x(y|\theta) - F_x(-y|\theta) = F(y + \theta) - F(-y + \theta) = m_f^*(\theta|y). \quad (7)$$

$F_x()$ denotes the distribution function when x is the random variable. (Eq.(7) also yields the well known property that the (derivative) density of $F_r^*(y|\theta)$ equals the sum of F_x densities, $f_x(y + \theta) + f_x(-y + \theta)$.)

$F_r^*(y|\theta)$ is shown in the Figure 4(a) (undarkened) curves for various θ . Intersections occur at every point (y, F_r^*) , unlike in the Section 2 joined RD's, since the transformation into y is non- 1-1 for all x . The fiducial dual $m_f^*(\theta|y)$, shown in the Figure 4(b) (undarkened) curves for various y , is non-monotone.

Since each intersection consists of two θ RD's, m^* has for each y a maximum value, at an intermediate θ_M say, given by $F_r^*(y|\theta_M)(\equiv F_M^*(y))$. In fact, equating to zero the derivative (density) of m^* yields the formula

$$\begin{aligned} \theta_M &= -\ln\left(\frac{\sinh y}{y}\right) \approx -\frac{y^2}{6} + \frac{y^4}{180}, \\ F_M^* &= F(y + \theta_M) - F(-y + \theta_M). \end{aligned}$$

The dashed curve in Figure 4(a) for $F_M^*(y)$ represents the envelope beyond which RD probabilities will not occur. The values shown for θ_M correspond to the maxima in the Figure 4(b) FM's.

$F_r^*(y|\theta)$ equals the area subtended under the EVD density $f(x)$ by the variable interval $(-y + \theta, y + \theta)$ with θ fixed, as y varies from $y = 0$ and $F_r^* = 0$ at the EVD mode ($x = 0$), to $y = \infty$ and $F_r^* = 1$. Similarly, $m^*(\theta|y)$ is the subtended area of the same interval, but now with y fixed and θ variable from $-\infty$ to $+\infty$. Because of the EVD left skewness, with density fall-off from the mode that is steeper in the positive θ direction than the negative θ direction, the subtended area $(-y, +y)$ at the mode is increased when θ is decreased until the (negative) maximum θ_M is reached. As y is increased θ_M becomes more negative. For a symmetric density θ_M remains at the zero mode for all y .

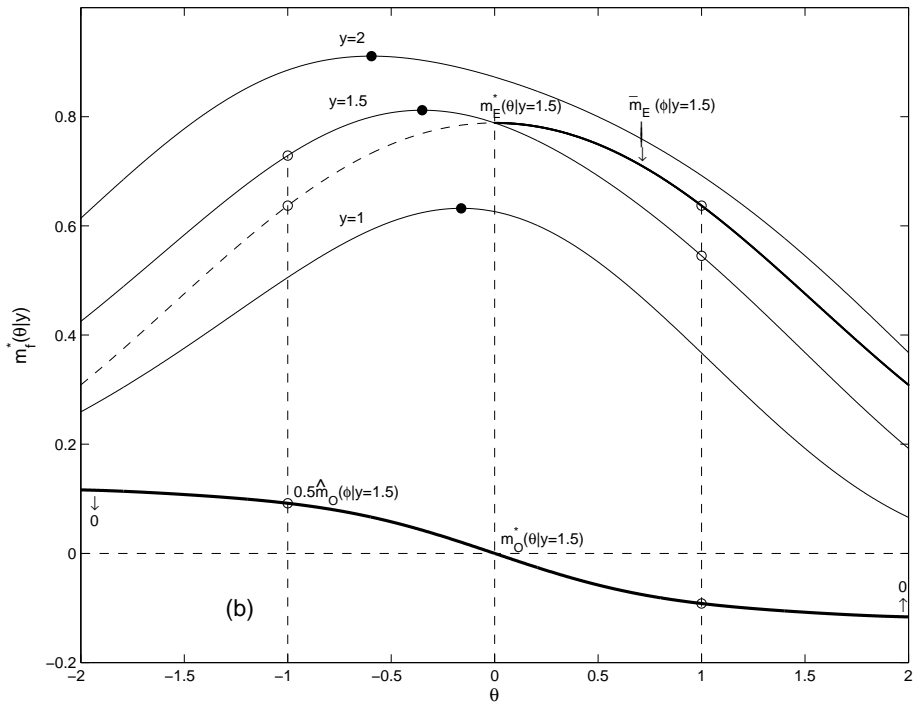
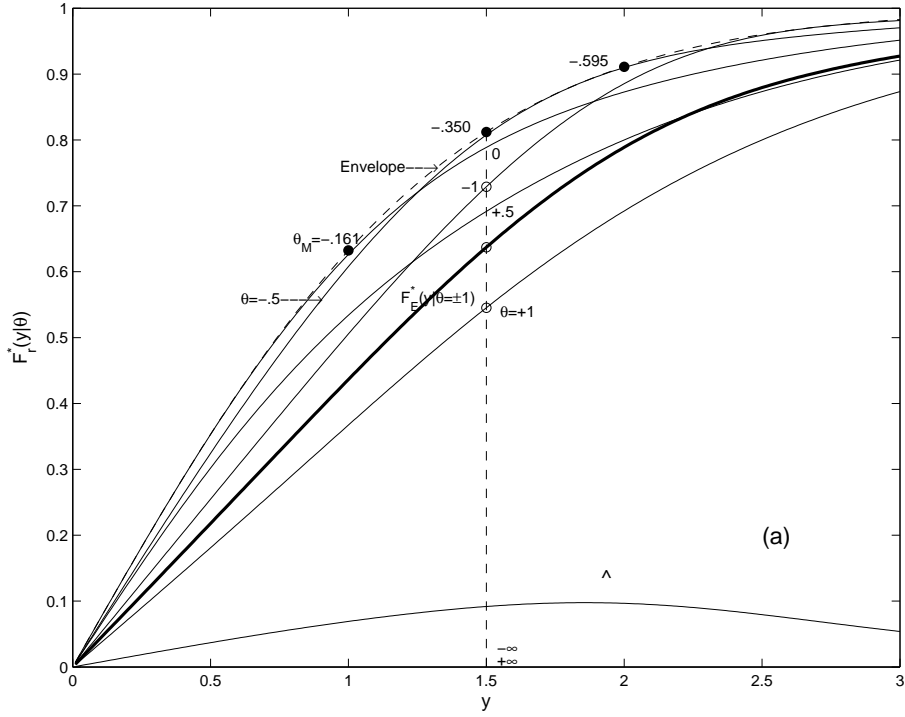


Figure 4: Composite I for EVD (a) $F_r^*(y|\theta)$ (b) $m_f^*(\theta|y)$

This *density subtended area* procedure has various applications, for example, in demonstrating existence of an intersection at every value of the RD: For each $y_0 > 0$ and (negative) $\theta_0 < \theta_M$ and with the corresponding area of (say) $A_0 (\equiv F^*(y_0|\theta_0))$ subtended by $(-y_0 + \theta_0, y_0 + \theta_0)$, there exists a unique θ'_0 with area A_0 subtended by the interval $(-y_0 + \theta'_0, y_0 + \theta'_0)$. This procedure also shows that a density with multiple modes results in multiple θ intersections.

The dual relation between the RD and FM is illustrated by the vertical line in Figure 4(a) for $y = 1.5$, and the corresponding $m^*(\theta)$ curve in Figure 4(b). Starting at $\theta = -\infty$ with $F_r^* = 0$ (the base line in Figure 4(a)), increasing θ yields increasing values of F_r^* as shown for $\theta = -1$ and -0.5 , until the maximum F_M^* at $\theta_M = -0.35$ is reached; this maximum is shown also in the Figure 4(b) $m^*(\theta|y = 1.5)$ curve. Further increase in θ to 0, +1 and $+\infty$ decreases F_r^* and m^* , ultimately to zero.

The composite variable ϕ and its composite distribution will be treated in Section 5.3 together with the related darkened curves in Figures 4(a) and 4(b), after analyzing the normal distribution situation.

Reciprocal distributions

A *reciprocal distribution* is obtained by interchanging variables (y, θ) with (ϕ, x) . Since the FD $F_f(\theta|x)$ is the same EVD as the RD, Eq.(7) yields also a reciprocal fiducial composite distribution of $\phi \equiv |\theta|$, denoted by $F_f^{*R}(\phi|x)$. This distribution is identical to the RD's in Figure 4(a), but now with ϕ as the abscissa and with x replacing θ . That is,

$$F_f^{*R}(\phi|x) = F(\phi + x) - F(-\phi + x).$$

Likewise the dual reciprocal random composite, $m_r^{*R}(x|\phi)$, is identical to the curves in Figure 4(b), with the same interchange of variables and hence also with the same equation above.

5.2 Normal distribution composite

For the normal distribution, $N(x + \theta)$, the RD $F_r^*(y|\theta)$ of the composite y is also given by Eq.(7) with N replacing F , and is shown in Figure 5(a).

The previous EVD intersections have now come together so that the RD for each $-\theta$ coincides with the RD for $+\theta$. (This follows from the symmetry condition, $N(-u) = 1 - N(u)$, applied to Eq.(7).) Thus these are weak intersections (defined in Appendix B), and the dual $m_f^*(\theta|y)$ curve in Figure 5(b) (including both the left dashed part and the right solid part) is non-monotone and symmetric about the maximum at $\theta = 0$; the maxima are represented also by the (dashed) RD envelope $F_r^*(y|0)$ in Figure 5(a).

The RD coincidences in Figure 5(a) imply that the RD's can be expressed as a function of the *composite-reducing* parameter $\phi \equiv |\theta|$. The RD's are now *composite-reduced* distributions $\bar{F}_r(y|\phi)$. They have become non-intersecting and, being bounded by the $\theta = 0$ maximum RD $\bar{F}_r(\phi|0)$, they are also incomplete. The dual FM $\bar{m}(\phi|y)$ in Figure 5(b) consists of the solid $+\theta$ portion of $m_f^*(\theta|y)$, with the abscissa parameter θ now replaced by ϕ ; i.e. $\bar{m}(\phi|y) = m^*(+\phi|y)$, $\phi \geq 0$. This FM is monotone, in accordance with Theorem 1, the equation being

$$\bar{m}(\phi|y) = N(\phi + y) - N(\phi - y), \quad \phi, y \geq 0. \quad (8)$$

The \bar{F}_r RD's in (relabelled) Figure 5(a) decrease in magnitude as ϕ increases; that is, ϕ is a decreasing parameter, whether θ is initially represented as increasing or decreasing. Hence the dual $\bar{m}(\phi|y)$ in (relabelled) Figure 5(b) is also monotone decreasing, from $\phi = 0$ and $\bar{m}(0|y) (= \bar{F}_r(y|0))$, to $\phi = +\infty$ and $\bar{m}(+\infty|y) = 0$. By defining $\bar{\mu}_f(\phi|y) \equiv 1 - \bar{m}_f(\phi|y)$, with initial value $\bar{\mu}_f(0|y) = 2N(-y)$, we can obtain a more useful representation as a monotone increasing *truncated* distribution*. [The * indicates a terminology different from that for normalized truncated distributions. An alternative (albeit oxymoronic) terminology that emphasizes its relation to the RD completeness condition is “incomplete FD”.]

The RD-FM relation can be summed up as: The composite-reduced RD's are non-

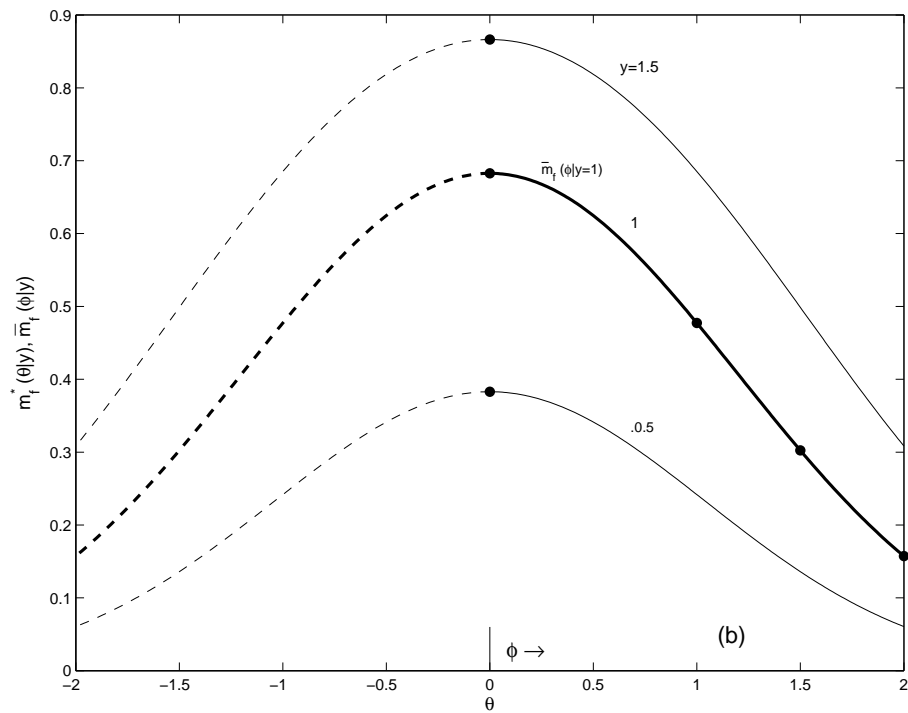
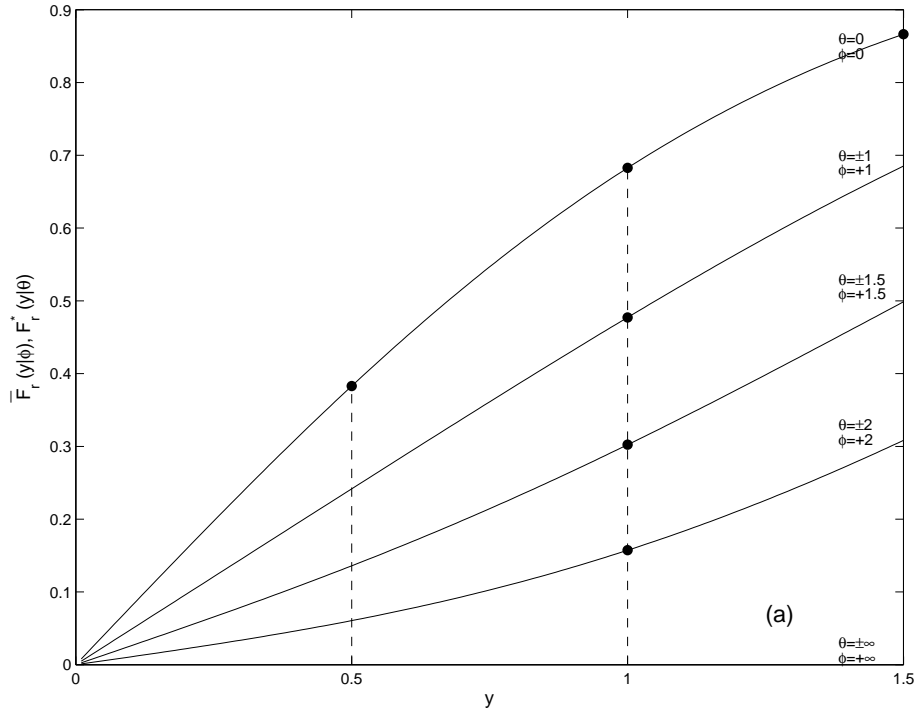


Figure 5: Composite for N.D. (a) $F_r^*(y|\theta)$ and $\bar{F}_r(y|\phi)$ (b) $m_f^*(\theta|y)$ and $\bar{m}_f(\phi|y)$

intersecting and incomplete iff the dual FM's are monotone and truncated*. The equivalence Eq.(4) yields also: $F_r^*(y|\theta)$ is composite-reducible iff the dual $m_f^*(\theta|y)$ is symmetric for all y .

These results apply to any (density) unimodal symmetric translation distribution $F(x + \theta)$. For multiple modes (local density maxima), $\bar{m}(\phi|y)$ is not monotone whence (Theorem 1) $\bar{F}(y|\phi)$ has intersections.

We note that $\bar{m}(\phi)$ is not the composite *distribution* of the composite variable ϕ , but is the FM that corresponds to the reduction of the RD $F_r^*(y|\theta)$, from a function of θ to an equivalent reduced representation as a function of ϕ . Appendix C shows that the composite *distribution* of ϕ is in fact identically zero.

The preceding analyses, which are applicable in essence also to non-translation parameters, indicate the likely truth of the conjecture that composite distributions are non-FD. Also indicated is that reduced-composite distributions are directly related to the completeness condition (ii) in the FD definition and in Theorem 2 of Section 3. Incomplete non-intersecting RD's apparently arise only from association with the envelope that exists for the non-FD RD's. (The completeness condition (ii) in the FD definition should perhaps be accompanied by a statement to that effect.)

Of course, a complete answer would consist of necessary and sufficient conditions for existence of incomplete/truncated* distributions.

Reciprocal distribution and fiducial counterexample

The reciprocal distribution of ϕ is obtained by starting with the FD $N(x + \theta)$ and then applying Eq.(7) as was done for y . The resulting distribution is also the same and is represented in Figure 5(a) with variables interchanged. The equation is:

$$F_f^{*R}(\phi|x) = N(\phi + x) - N(-\phi + x) = m_r^{*R}(x|\phi).$$

The coincidence of $+x$ and $-x$ curves in the relabeled Figure 5(a) marks these curves as being *reciprocal incomplete composite-reduced* fiducial distributions of ϕ , $\bar{F}_f^R(\phi|y)$,

with y the reducing-composite variable. The duals, $\bar{m}_r^R(y|\phi)$, are represented by the solid portions of the relabeled curves in Figure 5(b). We have then two fiducials for ϕ : (1) the dual truncated* distribution given by (with (derivative) density $f_f()$ included):

$$\begin{aligned}\bar{\mu}_f(\phi|y) &= 1 - [N(y + \phi) - N(-y + \phi)] = N(-y + \phi) + N(-y - \phi) \\ f_f(\phi|y) &= n(-y + \phi) - n(-y - \phi) = \sqrt{2/\pi}e^{-(y^2+\phi^2)/2} \sinh(y\phi);\end{aligned}$$

(2) the reciprocal incomplete distribution:

$$\begin{aligned}\bar{F}_f^R(\phi|y) &= N(y + \phi) - N(y - \phi) \\ f_f^R(\phi|y) &= n(y + \phi) + n(y - \phi) = \sqrt{2/\pi}e^{-(y^2+\phi^2)/2} \cosh(y\phi).\end{aligned}$$

Since $n(y - \phi) = n(-y + \phi)$, this last equation is also the density $f_r(y|\phi)$ of the RD $\bar{F}_r(y|\phi)$.

The two fiducials are relevant to Stein's counterexample [11]. Stein considered the RD of the n degree-of-freedom non-central chi-square (composite) distribution, $F_r(z|\psi)$, of $z = x_1^2 + \dots + x_n^2$ with non-centrality parameter $\psi = \theta_1^2 + \dots + \theta_n^2$. For $n = 1$ with $z = x^2, \psi = \theta^2$, the distribution is equivalent to the distribution of the 1-1 continuous transformation variables $|x| = \sqrt{z}$ and $|\theta| = \sqrt{\psi}$, which were treated above. Stein determined the approximate probability that the one-sided confidence interval for ψ will cover the true ψ , estimated for large n from the approximating normal distribution with the same mean and variance. The probability of covering this same parameter was estimated also for a fiducial confidence interval using a similar normal distribution approximation. The resulting large difference in coverage probabilities between the random and fiducial limits indicated a serious deficiency in the latter.

The reason for the difference was the use of the (n sample version) reciprocal rather than the dual fiducial distribution, so that the analysis actually confirms the non-equivalence between the reciprocal fiducial distribution and the random distribution. Stein does remark that "a more reasonable fiducial distribution leads to intervals based on ... confidence intervals."

In the absence of a fiducial framework, selecting the reciprocal fiducial – apparently the choice also of R.A. Fisher – may have been influenced by its equation being identical to the RD, a feature previously noted for translation-related FD's and RD's.

A criticism of Stein's probability analysis in this example has been given by Pinkham [9].

5.3 EVD Composite II: Composite distribution of ϕ

Previously obtained for the EVD were the asymmetrical FM's and RD's, $m_f^*(\theta|y)$ ($\equiv m^*(\theta)$ for brevity) and $F_r^*(y|\theta)$, shown in Figures 4(b) and 4(a). The determination of the composite *distribution* of ϕ from non-monotone $m^*(\theta)$ uses the fact that an arbitrary function can be uniquely represented as the sum of its even (E) and odd (O) component functions. For $m^*(\theta)$ we have

$$\begin{aligned} m^*(\theta) &= m_E^*(\theta) + m_O^*(\theta) \\ m_E^*(\theta) &= [m^*(\theta) + m^*(-\theta)]/2 \\ m_O^*(\theta) &= [m^*(\theta) - m^*(-\theta)]/2. \end{aligned}$$

m_E^* is symmetric; m_O^* is referred to as *opposite*.

Plotted (darkened) in Figure 4(b) for $y = 1.5$ are m_E^* and m_O^* . The circular dots at $\theta = +1$ and -1 illustrate the above equations: m_E^* is the average of the $\pm\theta$ values of m^* , and m_O^* is one-half the difference of the two curves (or $= m^*(-\theta) - m_E^*(-\theta)$). The negative values for $m_O^*(+\theta)$ are associated with m^* being a signed measure and reflect the positive skewness of the EVD. The above equations for m_E^* and m_O^* yield

$$m_E^*(\theta|y) = [F(y + \theta) - F(-y + \theta) + F(y - \theta) - F(-y - \theta)]/2. \quad (9)$$

$$m_O^*(\theta|y) = [F(y + \theta) - F(-y + \theta) - F(y - \theta) + F(-y - \theta)]/2. \quad (10)$$

These are also the equations of the RD duals, $F_E^*(y|\theta)$ and $F_O^*(y|\theta)$.

$F_E^*(y|\theta)$, shown (darkened) for $\theta = \pm 1$ in Figure 4(a), is the average of RD's $F_r^*(y| + \theta)$ and $F_r^*(y| - \theta)$. Similarly, F_O^* equals one-half the difference between these

two RD's (equivalently, equals $F_r^*(y|\theta) - F_E^*(y|\pm\theta)$) and is shown in Figure 4(a) for $\theta = -1$; $F_O^*(y|\theta)$ is identical but with negative values. (Note that F_O^* is a non-monotone distribution.)

F_E^* can also be obtained by replacing the EVD $F(x)$ by its density $f(x)$. The replaced symmetric even component density f_E is then obtained from the even-odd decomposition of f , namely, as the average of $f(x)$ and its reflection $f(-x)$: $f_E(x) = [f(x) + f(-x)]/2$. The corresponding RD is

$$F_E(x) = \int_{-\infty}^x f_E(\bar{x})d\bar{x} = [1 + F(x) - F(-x)]/2.$$

The composite is then

$$F_E^*(y|\theta) = F_E(y+\theta) - F_E(-y+\theta) = \frac{1 + F(y+\theta) - F(-y-\theta)}{2} - \frac{1 + F(-y+\theta) - F(y-\theta)}{2},$$

which reduces to Eq.(9). Similarly, with $f_O(x) = [f(x) - f(-x)]/2$ (a signed density), $F_O^*(y|\theta)$ reduces to Eq.(10).

As in the normal distribution, $F_E^*(y|\pm\theta)$ is a composite-reduced distribution $\bar{F}_E(y|\phi)$. The composite-reduced dual $\bar{m}_E(\phi|y)$ is shown in Figure 4(b) as the darkened positive half of $m_E^*(\theta|y)$.

The configurations for $F_E^*(y|\pm\theta)$ and $m_E^*(\theta|y)$ for varying θ and y are, since the density f_E is unimodal, qualitatively the same as in Figures 5(a) and 5(b) for the normal distribution.

Since m^* has an m_O^* component in addition to the symmetrical m_E^* component, F_r^* cannot, according to a previous necessary and sufficient condition, be represented as a composite-reduced RD.

The composite distribution, $\hat{m}(\phi)$, of the composite ϕ can be determined from its equality to the sum of its even and odd composites:

$$\hat{m} = \hat{m}_E + \hat{m}_O. \quad (11)$$

It is proven in Appendix C that $\hat{m}_E(\phi) = 0$ and $\hat{m}_O(\phi) = 2m_O(+\theta)$ (or $= 2m_O(-\theta)$) when $m_O(-\theta)$ is the positive half). Hence $\hat{m}(\phi) = \hat{m}_O(\phi)$.

The positively valued $m_{\mathcal{O}}^*(-\theta)$ in Figure 4(b) represents $0.5\hat{m}_{\mathcal{O}}(\phi)$. The dual signed RD $F_{\mathcal{O}}^*(y|\theta)$, shown in Figure 4(a) for $\theta = -1$, represents also $.5\hat{F}_r(y|\phi)$.

The following summarizes the properties of the odd distribution-composite in comparison with the even reduction-composite.

- $\bar{m}_E(\phi) = m^*(+\theta)$ and $\hat{m}_E = 0$; $\hat{m}_{\mathcal{O}} = 2m^*(\pm\theta)$ and $\bar{m}_{\mathcal{O}}$ does not exist;
- $F_E^*(y|+\theta) = F_E^*(y|-\theta)$ (coincident); $F_{\mathcal{O}}^*(y|+\theta) = -F_{\mathcal{O}}^*(y|-\theta)$ (opposite);
- $m_E^*(+\theta|y) = m_E^*(-\theta|y)$ (symmetric); $m_{\mathcal{O}}^*(+\theta|y) = -m_{\mathcal{O}}^*(-\theta|y)$ (opposite);
- f_E density symmetric; $f_{\mathcal{O}}$ density opposite;
- For unimode f , $\bar{F}_E(y|\phi)$ is non-intersecting; $\hat{F}_{\mathcal{O}}(y|\phi)$ is intersecting (since $\hat{m}_{\mathcal{O}}^*(\phi)$ is non-monotone with a maximum).

We note finally the relation:

$$m(+\theta) = m_E(+\theta) + m_{\mathcal{O}}(+\theta) = \bar{m}_E(\phi) + 0.5\hat{m}_{\mathcal{O}}(\phi).$$

Remarks on before vs. after observation

The previous sections have dealt with the equivalence between the RD and FD representations: $F_r(x|\theta)$ for all θ equals $F_f(\theta|x)$ for all x . The difference in emphasis – given x vs. given θ – is related to their roles in applications. When an actual observation x_0 occurs, the relevant information for inference is the single FD $F_f(\theta|x_0)$. Prior to the observation there is only the RD probability outcomes $F_r(x|\theta)$ for all possible observations x and for each θ .

In practice this before-after distinction may not always be sharp. In hypothesis testing the FD representation corresponding to the (non-observed) critical value for acceptance is useful. The opposite may also occur, as in confidence limits when the appropriate θ RD can be selected after the observation occurs. A difference arises when

the RD and FD criteria are not the same, as in the significance test for the Behrens-Fisher problem. It is interesting that Laplace in a 1777 paper made a before-after distinction when discussing “the search for the [proper] mean”. Laplace states (Stigler [8, p.119]):

The problem ... may be regarded from two different points of view, depending on whether we consider the observations before or after they are made... It is from the first of these viewpoints that the question has, prior to now, been treated ... However ingenious their researches have been, they can only be of very little use to observers.

Laplace’s “observers” refers to “geometers”, such as astronomers, who utilize the observations.

APPENDIX A: Comparison of pivotal quantity (PQ) formulation and geometric formulation

More detailed analyses are given in a concomitant paper on fiducial applications. A summary appears at the end of this Appendix.

A1. Single observation

It is convenient to divide PQ's into *PQ1 translation parameters* and *PQ2 general (non-translation) parameters*.

PQ2 general parameter formulation

As noted by Seidenfeld [10, p.362], the PQ2 defining equation that is considered the natural extension of PQ1 pivoting, is

$$F(x, \theta) = \beta. \tag{12}$$

In the present context β is the confidence coefficient associated with a one-sided confidence limit (either an upper limit or a lower limit). The PQ2 Eq.(12) is represented in Figure 1 by a horizontal line (a plane in the three dimensional surface), say $F(\equiv F_b) = \beta$. This line intersects each θ RD in an $x(\equiv x_b(\theta))$ given by $F_r(x_b|\theta)(\equiv \Pr(X \leq x_b|\theta)) = \beta$. When the RD's are strictly non-intersecting $x_b(\theta)$ is a strictly monotone function which can be inverted to yield the *confidence limit function* $\theta_b(x)$.

In terms of random probability

$$\Pr(\theta_b(X) < \theta|\theta) = \beta. \tag{13}$$

This equation constitutes the (non-fiducial) random probability representation of the confidence limit function, which is analyzed in more detail in Cramér [12, pp. 510-512]. Cramér's analysis of the inverting (readily modified for a one-sided limit) considers the probability equivalence of the sets corresponding to $x_b(\theta)$ and $\theta_b(x)$. These sets are related to the set of points $(x, \theta)_b$ of the fiducial surface that satisfy the PQ2 Eq.(12),

and which are represented as $x_b(\theta)$ in the RD θ sections and as $\theta_b(x)$ in the fiducial x sections. Their equality also constitutes the PQ2 formulation, represented by the *PQ2 confidence limit identity*:

$$\theta_b(x) = x_b(\theta). \quad (14)$$

This fiducial-oriented equation represents the inverting in Cramér’s non-fiducial random-oriented treatment of confidence limit.

Letting β vary from 0 to 1 yields the FD with $F_f(\theta_b|x) = \beta$; that is, the β confidence limit is the β percentile of the FD. Since $\theta_b(\equiv \theta(\beta))$ is strictly monotone for each x , the inverse function F_f^{-1} is defined and $\theta_b(x) = F_f^{-1}(\beta|x)$. Similarly, $F_r(x_b|\theta) = \beta$ and $x_b(\theta) = F_r^{-1}(\beta|\theta)$. Hence the identity Eq.(14) can be written also as an *inverse-FD identity*

$$F_f^{-1}(\beta|x) = F_r^{-1}(\beta|\theta). \quad (15)$$

This identity reflects, and is equivalent to, the fact that the PQ2 definition Eq.(12) relates to an “inverse function” (say) of $F(x, \theta)$, namely $F^{-1}(\beta) = (x, \theta)_b$.

Additional analysis of PQ2 is presented following the analysis of PQ1.

Geometric formulation

The FD, $F_f(\theta|x_0)$, corresponding to non-intersecting RD’s is obtained from the geometric identity Eq.(1). The confidence limit $\theta_b(x_0)$ in Figure 1 is, as noted above, the monotone representation of $(x_0, \theta)_b$ in the fiducial x_0 section – essentially the same as the inverting of $x_b(\theta)$ – and corresponds to the β percentile of the FD.

For the general case of possibly intersecting RD’s, we use the geometric identity Eq.(4) to define the fiducial measure M_f . The confidence limit(s) are, as before, obtained from the intersection with the horizontal plane, $F_b = \beta$, and yield the set $(x, \theta)_b$. For each x there may be multiple θ values, say $\theta_i(x)$, which we denote by the set $\underline{\theta}(\equiv \underline{\theta}(x))$. Thus, we can write the geometric identity Eq.(4) as

$$M_f(\underline{\theta}|x) = F_r(x|\underline{\theta}) = \beta,$$

which is interpreted as applying to each $\theta_i \in \underline{\theta}$. $\underline{\theta}$ then represents the “confidence limit set”. We consider three cases:

(1) $\underline{\theta}$ is a single unique $\theta_1(\equiv \theta_1(x))$. M_f is then a strictly monotone FD F_f and (iff) the RD’s are strictly non-intersecting. This is the usual situation in applications, also assumed for the PQ2 solution.

(2) The FD is non-strict and contains a constant interval, $\underline{\theta} = [\theta_1, \theta_2]$, of admissible confidence limits. The RD’s are touching at x_0 (say), and $\theta_b(x)$ is monotone but not continuous, with a jump at x_0 . Some (inequality) modifications are required in case (1) analyses.

(3) $M_f(\equiv m_f)$ is non-monotone corresponding to intersecting RD’s. Multiple ”confidence limits” are obtained, with $\theta = \theta_1, \theta_2, \dots$. This case does not arise in applications.

PQ1 translation parameters

[Much of the following analysis for a strict translation parameter can be extended to generalized translation parameters, generated by three strictly monotone functions. For brevity the general class is also referred to as translation-scale.]

The pivotal quantity $u \equiv (x + \theta)$ was early recognized as a significant quantity with a pivoting property that yields both the random and the fiducial distributions. PQ1 defines $F(x, \theta)$ in terms of u and its probability distribution $F^*(u)$:

$$F(x, \theta) = F^*(x + \theta) \equiv F^*(u). \quad (16)$$

(When $F^*(u)$ is a probability distribution the RD’s are non-intersecting.) This equation also defines a translation parameter as being equivalent to existence of a PQ1 pivot.

For the RD we have

$$F_r(x|\theta) = F^*(\underline{x} + \theta), \quad (17)$$

where \underline{x} indicates that the pivot is on x . A pivoting, and with $x = x_0$, gives the FD, and also the PQ1 formulation,

$$F_f(\theta|x_0) = F^*(x_0 + \underline{\theta}). \quad (18)$$

Note that the FD is obtained merely by interchanging x and θ in the RD. Fisher in his book [3, pp. 52-54] illustrates the “fiducial argument” by using a similar interchange in an exponential distribution with scale parameter.

It is readily verified that the FD density of Eq. (18) is identical to the bayesian posterior distribution that is obtained when using the non-informative uniform prior distribution applied to the RD density of Eq. (17).

The PQ1 formulation is also a geometric formulation. In fact, the same right sides of Eq.(17) (with $x = x_0$) and Eq. (18) gives the geometric identity.

The PQ1 relation for the (strict) translation parameter can be extended to generalized translation-scale parameters. In this family each FD is identical to a posterior distribution with a corresponding non-informative prior, such as $1/\theta$ for a scale parameter θ . Thus there is an (iff) equivalence relation between a PQ1 pivot, a translation-scale parameter, and a bayesian-non-informative solution.

PQ2 extension of PQ1

It is natural to extend the translation parameter’s PQ1 pivoting to non-translation-scale parameters. This has been accomplished by a general PQ definition wherein the right side of Eq.(16) is replaced by the $[0,1]$ uniform distribution, as in the PQ2 definition Eq.(12).

The resulting properties of PQ2 differ considerably from PQ1. PQ1 has a real pivot with formulation identical to the geometric formulation. PQ2’s pivoting, on the other hand, is accomplished by monotone inverting, which results in the FD-inverse formulation. The PQ2 definition, which specifies the $(x, \theta)_b$ values for each β , is equivalent to the “inverse” of $F(x, \theta)$ and the resulting confidence limit, while PQ1 defines a general $F^*(u)$ that ranges over all values of F and yields the FD directly.

PQ2 is not a pivoting extension of PQ1; equivalently, PQ1 is not a special case of PQ2. Most likely, a PQ1 extension with a pivoting property does not exist. A similar and closely related translation-scale situation is the non-informative property

of a prior distribution which cannot be extended to non-translation-scale parameters. Non-extension of pivoting is also related to the pivot in PQ1 serving as an equivalent definition of a translation parameter. Note, however, that the general geometric formulation is a *non-pivoting* extension of PQ1's geometric formulation property.

Even more troubling is the fact that PQ2's inverse FD formulation – which has some merit for a single observation in being equivalent to the direct random distribution determination of confidence limits – is not generalizable to multiple observations (treated in the next section). The situation is analogous to defining a probability distribution in terms of its inverse, and then attempting to extend the inverse definition to the probability distribution of two variables or to a conditional probability distribution. Although perhaps not impossible, implementing any such extension would undoubtedly be very difficult and, furthermore, unnecessary.

The principal conclusions are: (i) The PQ2 formulation is inappropriate and should not be used. (ii) The PQ1 pivot defines a generalized translation-scale parameter and is also a geometric formulation. (iii) The geometric formulation is applicable to all parameters and to both single and multiple observations.

A2. Geometric formulation derivation of FD for multiple observations

For simplicity we assume only two independent observations; the proof for the general case is essentially the same. Initially we suppose that the parameters are different: x_i has parameter θ_i with geometric identity

$$F_{f_i}(\theta_i|x_i) = F_{r_i}(x_i|\theta_i), i = 1, 2. \quad (19)$$

The joint geometric identity and joint FD are then the product

$$F_f(\theta_1, \theta_2|x_1, x_2) \equiv F_{f_1}(\theta_1|x_1) \cdot F_{f_2}(\theta_2|x_2) = F_{r_1}(x_1|\theta_1) \cdot F_{r_2}(x_2|\theta_2). \quad (20)$$

That is, θ_1 and θ_2 are the two parameter variables that define the joint FD function.

The desired FD, $F_f(\theta|x_1, x_2)$, is obtained when (i.e., conditional on) $\theta_1 = \theta_2 = \theta$ in the middle fiducial expression in Eq.(20): (For clarity the usual conditional symbol $|$ is replaced by $||$.)

$$F_f(\theta|x_1, x_2) \equiv F_f(\theta_1, \theta_2|x_1, x_2)||(\theta_1 = \theta_2 = \theta) = \{F_{f_1}(\theta_1|x_1) \cdot F_{f_2}(\theta_2|x_2)\}||(\theta_1 = \theta_2 = \theta). \quad (21)$$

For the right RD term in Eq.(20) the conditioning is achieved merely by substituting $\theta_i = \theta$. Substitution does not, however, give correct conditioning for Eq.(21). The correct result is most readily obtained using fiducial densities. The density equation, obtained from the derivatives of Eq.(20), merely replaces the cumulative F 's in Eq.(21) by density f 's:

$$\{f_f(\theta|x_1, x_2)d\theta \equiv f_{f_1}(\theta_1|x_1) \cdot f_{f_2}(\theta_2|x_2)d\theta_1 \cdot d\theta_2\}||(\theta_1 = \theta_2 = \theta). \quad (22)$$

Also needed is a *density geometric identity* – which is also Fisher's identity, the density version of Eq.(2) – that replaces Eq.(19) (with $\theta_i = \theta$):

$$f_{f_i}(\theta|x_i) = \frac{\partial}{\partial\theta} F_{r_i}(x_i|\theta) = \frac{\partial}{\partial\theta} \int_{-\infty}^{x_i} f_{r_i}(\bar{x}_i|\theta)d\bar{x}_i. \quad (23)$$

The conditioning in Eq.(22) is achieved, as shown below, by first substituting $\theta_i = \theta$. The two variable (θ_1, θ_2) density is carried into the one variable θ density. Likewise the two variable probability density element $d\theta_1 \cdot d\theta_2$ is carried into the one variable probability density element $d\theta$. We note, however, that the product of two densities (for the same variable) is not in general a density, i.e. with a total integral of unity, whence the product requires normalization by the value of the integral. The desired FD density should then be given by:

$$f_f(\theta|x_1, x_2)d\theta = \frac{f_{f_1}(\theta|x_1) \cdot f_{f_2}(\theta|x_2)d\theta}{\int_{-\infty}^{+\infty} f_{f_1}(\theta|x_1) \cdot f_{f_2}(\theta|x_2)d\theta}. \quad (24)$$

The proof of this equation uses the general conditional probability definition applicable to arbitrary sets A, B:

$$\text{Pr}'(A|B) = \frac{\text{Pr}'(A \cap B)}{\text{Pr}'(B)}.$$

The set A consists of arbitrarily selected pairs (θ_1, θ_2) , such as appears in Eq.(20); A is also the union of A_1 (where only $\theta_1 \neq \theta_2$) and A_2 (where only $\theta_1 = \theta_2 = \theta$). Set B consists of all possible values of $\theta \in [-\infty, +\infty]$, whence $\Pr'(B)$ equals the denominator of Eq.(24). Also, since $A \cap B = A_2 = \theta$ the probability (density) $\Pr'(A \cap B)$ is the numerator of Eq.(24). This completes the proof.

For n observations the FD density consists of: (i) obtaining the n fiducial densities f_{f_i} from f_{r_i} using the geometric identity density Eq.(23), and then (ii) obtaining the normalized product of the f_{f_i} 's.

The solution holds trivially for $n = 1$ where the normalizing denominator is unity; the solution becomes, after integrating, the geometric identity Eq.(1).

The β confidence limit corresponding to the solution is given by the β percentile of the cumulative FD, $F_f(\theta|x_1, x_2)$, the integral of Eq.(24). The procedure is similar to that for a single observation, and can yield also non-unique confidence limit solutions. For a strict translation parameter with pivot density $f^*(x + \theta)$, the fiducial solution, Eq.(23) and Eq.(24), will reduce to the bayesian posterior solution using the non-informative uniform prior, namely,

$$f_f(\theta|x_1, \dots, x_n) = \frac{\Pi f^*(x_i + \theta)}{\int_{\theta} \Pi f^*(x_i + \theta) d\theta}. \quad (25)$$

The equivalence follows from the fact that the derivative and integral in Eq.(23) are now inverses and hence cancel, yielding the defining density pivoting equation for a strict translation parameter:

$$f_r(x_i|\theta) = f^*(x_i + \theta) = f_f(\theta|x_i). \quad (26)$$

Equivalence with the bayesian solution can be shown to hold also for generalized translation-scale parameters.

We note the similarity between the form of the general (non-translation) fiducial solution Eq.(24), and the form of the bayesian solution Eq.(25). This suggests that the former can be described as a *fiducial-bayesian* solution. In fact, after the observations

$f_{r_i}(x_i|\theta)$ have been converted to $f_{f_i}(\theta|x_i)$ using Eq.(22), the calculations for the FD in Eq.(24) are identical to the calculations for the bayesian posterior distribution solution in Eq.(25) using a uniform prior.

Conclusions

The main conclusions from the preceding analyses are the following:

- The PQ formulation is satisfactory only for generalized translation-scale parameters where actual pivoting occurs; the resulting fiducial distributions are also identical to those obtained from the geometric formulation.
- For other parameters and a single observation the PQ formulation, which entails inverting rather than pivoting, yields the *inverse* of the fiducial distribution. This property is not useful for obtaining the fiducial distribution for multiple observations.
- For multiple observations, only the geometric formulation provides the fiducial distribution and associated confidence limits, a problem previously unsolved. For general translation-scale parameters this fiducial distribution reduces to the ordinary bayesian posterior distribution using a non-informative prior.

The geometric formulation remedies the flaw in the PQ formulation and should be considered the correct fiducial formulation. Preliminary investigation suggests that this formulation – besides yielding the iff result on existence of fiducial distributions and also the solution for multiple observations – can be expected to yield additional new results. This may well lead to increased acceptance of fiducial probability and recognition of its essential role in statistical theory and practice.

Fiducial applications paper

A related concomitant paper presents an overview of selected fiducial applications using the geometric formulation. Besides providing a more detailed treatment of confidence limits and FD's, other areas, especially significance tests, are addressed. In particular, it is shown that a null hypothesis is accepted if and only if the hypothesis lies within the upper (and/or lower) confidence limit. For sequential selection between two alternative hypotheses, an additional "no-difference" hypothesis is required; termination occurs when one of the three hypotheses satisfies the upper and/or lower confidence limit (the reverse of the limit for null hypotheses).

Other topics include a detailed treatment of PQ's, generalized translation parameters and bayesian solutions, and analysis of adjacent FD's.

Application of the geometric formulation to multiple parameters is expected to address the following topics: extension of the non-intersecting FD existence theorem; FD's and confidence regions for single and joint parameters; extension of Lindley's characterization of bayesian parameters; and optimality of significance tests. Also to be considered is the problem of non-unique PQ solutions that have been addressed especially by Savage and Tukey in [13].

APPENDIX B: Analysis of intersections

The proof of Theorem 1 in Section 3 yields also the following contrapositive theorem:

Theorem 1CP $M_f(\theta|x)$ is non-monotone for some $x(= x_0)$ say, iff $F_r(x|\theta)$ has an intersection for some x'_0 ($=$ or $\neq x_0$).

A better understanding of intersections can be gained from an independent proof of this theorem. Intersections, however, are more varied and complex than non-intersections and a complete analysis would exceed the scope of this paper. The preliminary analysis here will, however, lead to a proof of the above theorem.

It is useful to note the following three cases pertaining to right and left neighborhoods of x_0 , for two θ RD's which have x_0 as a common point, i.e., which satisfy condition (i): $F_r(x_0|\theta_1) = F_r(x_0|\theta_2)$. Condition (ii) for each case is:

(ii') touching: the same θ inequality in left and right neighborhoods; touching then applies to all θ in the interval $[\theta_1, \theta_2]$.

(ii'') ordinary intersection: opposite θ inequalities in left and right neighborhoods.

(ii''') weak intersection: equality in both left and right neighborhoods: $F_r(x-|\theta_1) = F_r(x-|\theta_2)$ and similarly for $x+$.

We also consider the mixed combination with equality (ii''') on one neighborhood side and inequality (ii'') on the other side.

The non-monotone (NM) contrapositive of the general monotone definition is:

Definition NM *$f(z)$ is a non-monotone function if there exist z_i ($i = 1, 2, 3, 4$) (not necessarily all different) such that $z_1 > z_2$ implies (say) $f(z_1) > f(z_2)$ and $z_3 > z_4$ implies $f(z_3) < f(z_4)$.*

The following theorem may serve as a more useful equivalent definition:

Theorem EQ/NM *A continuous function $f(z)$ is non-monotone iff there exist z' and z'' such that $f(z') = f(z'')$, provided that $f(z)$ is not constant on the interval $[z', z'']$.*

The proof of the theorem when $f(z)$ is non-monotone is essentially the same as in Theorem 1S where Lemma 1 is cited together with the various triplet cases of the $f(z_i)$. In the other direction (without continuity), there exists z_0 such that (say) $z' < z_0 < z''$; then the Definition NM conditions are satisfied for the pairs (z', z_0) and (z_0, z'') .

Ordinary intersection

We have the following

Proposition 1

$M_f(\theta|x_0)$ is non-monotone if a finite number $n(\geq 2)$ of RD's intersect at x_0 ; one may then take $x'_0 = x_0$ in Theorem 1CP.

In fact, we have $F_0 = F_r(x_0|\theta_i)(\equiv M_f(\theta_i|x_0))$, $i = 1, \dots, n$ but not for any $\theta^* \neq$ all θ_i . Theorem EQ/NM then applies.

In the Section 2 example the point labeled A in Figure 2(a) has three RD intersections at $x_0 = 1.25$; the corresponding $\theta_1, \theta_2, \theta_3$ are shown in the non-monotone FM of Figure 2(b). It is unnecessary to verify the intersection reverse inequalities (ii'') in the

right and left neighborhoods; if the inequalities were not reversed the RD's would be touching.

Proper interval intersection

Suppose that the number of intersections at x_0 is infinite, consisting of all θ 's in a θ interval $[\theta_1, \theta_2]$, which is assumed to be a proper subset of $[\theta_m, \theta_M]$. Since M_f is constant in the θ interval, we have the exceptional case in Theorem EQ/NM: M_f can be monotone when the two remaining segments, $[\theta_m, \theta_1]$ and $[\theta_2, \theta_M]$, are monotone (increasing, say).

This situation arises in the Section 2 example when $x_0 = x_T$, the boundary transition point between intersections and non-intersections (see Figure 2(a)). All transition RD's in the intersection region intersect at x_T , and the remaining RD's are increasing. The intersection inequality, together with the continuous variation with x of the RD's, implies that the left (say) neighborhood of x_T will be intersection-free with monotone M_f 's, while the right neighborhood will have intersections at any $x'_0 (> x_0)$ from RD's within the intersection region. These satisfy Proposition 1 and thus M_f is non-monotone.

Essentially the same argument applies when either, but not both, $\theta_1 = \theta_m$ or $\theta_2 = \theta_M$.

The above remarks yield

Proposition 2

(a) *If the intersections at x_0 do not consist of a single interval then $M_f(\theta|x_0)$ is non-monotone.*

(b) *If the intersections at x_0 consist of a single interval then there is an x'_0 in the right or left neighborhood of x_0 where $M_f(\theta|x'_0)$ is non-monotone.*

Equivalently, (a) is 'iff' whence (b), also 'iff', is the contrapositive of (a).

Complete interval intersection

When all θ RD's in the complete (finite) interval $[\theta_m, \theta_M]$ intersect at x_0 , then

$F_r(x_0|\theta) = \text{constant} = M_f(\theta|x_0)$ for all θ and hence are trivially monotone (with unspecified θ direction). Since no RD's remain to provide intersections in a neighborhood, monotones in θ can exist, in opposite directions, for each side of x_0 . Thus the intersection at x_0 may not lead to a non-monotone M_f for any $x'_0 \neq x_0$, seemingly counter to Theorem 1 (or Theorem 1CP).

As noted previously, this *endpoint solution* may in fact arise, where x_0 becomes a common endpoint, after normalization, for two adjacent FD's. However, the solution is not applicable to Theorem 1 (or Theorem 1CP) which implicitly requires a single fiducial model with zero-one RD endpoints.

Weak intersection

Suppose the θ_1 and θ_2 RD's satisfy an equality $F_r(x|\theta_1) = F_r(x|\theta_2)$ not only for $x-$ and $x+$ in left and right neighborhoods of x_0 , but also when these neighborhoods encompass the entire domain. The θ_1 and θ_2 RD's then completely coincide for all x . Since $M_f(\theta_1|x) = M_f(\theta_2|x)$, it follows that M_f is non-monotone for all x and the RD's have a so-called *weak intersection*.

An example appears in Section 5, Figures 5(a) and 5(b), where weak intersection coincident RD pairs are obtained for each $\pm\theta$.

Weak intersection coincidence can be extended to a finite number of θ 's. However, an extension to a θ interval, with accompanying constant FM, yields a non-intersection touching interval.

In view of Proposition 2, Proposition 1 can now be strengthened to

Proposition 1* $M_f(\theta|x_0)$ is non-monotone iff there are ordinary or weak RD intersections at x_0 .

(This proposition assumes that it is not admissible to have two disjoint interval intersections at x_0 , or a single interval intersection plus discrete intersections.)

An *intermediate weak intersection* has a restricted coincidence, i.e. the neighborhood equalities hold only for the interior of a limited intersection x -segment, $[x_1, x_2]$;

also the inequality in the left neighborhood of x_1 is the opposite of the inequality in the right neighborhood of x_2 . At the endpoints will be an ordinary intersection while at interior x 's one has weakly intersecting RD's.

A number of areas require further investigation, including θ additions and removals in an x -segment; also whether intersecting θ RD's can be replaced by touching θ -intervals. The various uncertainties associated with intersections do not, however, affect the following proof of Theorem 1CP, which essentially combines the previous results.

Proof of Theorem 1CP: Suppose there are intersections at x_0 with $F_r(x_0|\theta) = F_0 (= M_f(\theta|x_0))$ for all θ in a closed set Θ . (a) If Θ is not an interval then there exist at least two θ 's, say θ_1, θ_2 , such that $M_f(\theta_i|x_0) = F_0$ ($i = 1, 2$), and also other θ 's in the interval $[\theta_1, \theta_2]$ that are not equal to F_0 . Theorem EQ/NM then states that M_f is non-monotone. (b) If Θ is an interval (and a proper subset of $[\theta_m, \theta_M]$) with $M_f(\theta|x_0) = \text{constant}$ for all θ in Θ , one has a (proper) θ -interval intersection. In a neighborhood of x_0 there will then exist an x'_0 with non-interval intersections and non-monotone $M_f(\theta|x'_0)$.

Conversely, suppose there exists an x_0 and an FM such that $M_f(\theta|x_0)$ is non-monotone. Then there exist at least two (non-touching) θ_i such that $M_f(\theta_1|x_0) = M_f(\theta_2|x_0)$ and not contained in an intersecting θ -interval. Hence the θ_i RD's must be intersecting. ■

APPENDIX C: Proof for composite distributions

This appendix derives the distributions for \hat{m}_E and \hat{m}_O in Eq.(11). The proof uses the theorem, proven in [5, Theorem 4.4, p. 231], that a non-monotone function, such as $m_E^*(\theta')$ in Figure 4(b), can be represented as the difference of two monotone functions, $\mathcal{M}_1(\theta')$ and $\mathcal{M}_2(\theta')$ with $\mathcal{M}_1(\theta') - \mathcal{M}_2(\theta') = m_E^*(\theta')$. (In the following it is convenient to let θ have positive values only, with negative values denoted by $-\theta$); otherwise (as

in the above equation) θ' is used. In some equations either θ or θ' is acceptable.)

An example of the construction, such as for $m_E^*(\theta')$, adjoins to the increasing negative half $m_E^*(-\theta)$ at its maximum value at $\theta = 0$ – equal, say, to $A \equiv m_E^*(0)$ – the reflection of the decreasing half $m_E^*(+\theta)$. This defines the monotone function $\mathcal{M}_1(\theta') = 2A - m_E^*(+\theta)$ for $\theta' > 0$, and $= m_E^*(-\theta)$ for $\theta' < 0$. We define also the monotone function $\mathcal{M}_2(\theta') = 2A - 2m_E^*(+\theta)$ for $\theta' > 0$ and $= 0$ for $\theta' < 0$. Then $\mathcal{M}_1(\theta') - \mathcal{M}_2(\theta') = m_E^*(\theta')$, as required.

Applying Eq.(6) to \mathcal{M}_1 and \mathcal{M}_2 , the difference then yields $\hat{m}_E = \hat{\mathcal{M}}_1 - \hat{\mathcal{M}}_2$. In fact, the right and left probabilities about zero are $R_i = \mathcal{M}_i(+\theta) - \mathcal{M}_i(0)$ and $L_i = \mathcal{M}_i(0) - \mathcal{M}_i(-\theta)$, which gives then $\hat{\mathcal{M}}_i = R_i + L_i$.

For m_E^* we have

$$\begin{aligned} R_1 &= A - m_E^*(+\theta), \quad L_1 = A - m_E^*(-\theta), \quad \hat{\mathcal{M}}_1 = 2A - 2m_E^*(\theta), \\ R_2 &= 2A - 2m_E^*(+\theta), \quad L_2 = 0, \quad \hat{\mathcal{M}}_2 = 2A - 2m_E^*(\theta), \end{aligned}$$

whence $\hat{m}_E^* = [\mathcal{M}_1 - \mathcal{M}_2](\theta) = 0$.

The general bounded variation construction in [5] for the \mathcal{M}_i is specialized here for a continuous (non-monotone) function $m(\theta')$ with alternating increasing and decreasing segments. The monotone increasing construction for \mathcal{M}_1 is obtained by reflecting each monotone decreasing segment, which is then joined monotonically to the preceding increasing segment. \mathcal{M}_2 is constant at the increasing segments and equal in magnitude to twice each reflected decreasing segment (as in the above m_E^* example), and with all segments joined monotonically. The result is $\mathcal{M}_1 - \mathcal{M}_2 = m(\theta')$.

This construction has a signed measure interpretation where the positive measure \mathcal{P} corresponds to increasing m and negative measure \mathcal{N} corresponds to decreasing m , with the change occurring at each local maximum or minimum. Then $\mathcal{M}_1 = \mathcal{P} + \mathcal{N}$ and $\mathcal{M}_2 = 2\mathcal{N}$, yielding the signed measure representation $m = \mathcal{M}_1 - \mathcal{M}_2 = \mathcal{P} - \mathcal{N}$.

Additivity of the signed measure and the \mathcal{M}_i enables one to alter the sequence of operations. Instead of $R_i + L_i = \hat{\mathcal{M}}_i$ and $\hat{m} = \hat{\mathcal{M}}_1 - \hat{\mathcal{M}}_2$, as in the above equations,

one can use:

$$\begin{aligned}
R_{1,2} &\equiv R_1 - R_2 = [\mathcal{M}_1 - A] - [\mathcal{M}_2 - 0] = [\mathcal{M}_1 - \mathcal{M}_2](+\theta) - A = m_E^*(+\theta) - A, \\
L_{1,2} &\equiv L_1 - L_2 = [A - \mathcal{M}_1] - [0 - \mathcal{M}_2] = A - [\mathcal{M}_1 - \mathcal{M}_2](-\theta) = A - m_E^*(-\theta), \\
\hat{m}_E &= R_{1,2} + L_{1,2} = 0.
\end{aligned}$$

Thus one need not obtain the actual equations for the \mathcal{M}_i , since the difference always equals the value of (non-monotone) $m(\theta')$. Note also the canceling of the non-zero value A. We remark also that the analysis is unaffected by an ordinate translation or reflection.

For the analysis of the odd function m_O^* in Figure 4(b) it is somewhat simpler to treat the reflected function $m_O(\theta') \equiv m_O^*(-\theta')$, so that the positive values appear for $+\theta$. To obtain \mathcal{M}_1 , the two decreasing segments are reflected: the segment $\theta' > \theta_M$ (where the $m_O(+\theta)$ maximum occurs) and the $\theta' < -\theta_M$ segment. For the unreflected monotone increasing segment, $-\theta_M < \theta' < +\theta_M$, we have $\mathcal{M}_1 = m_O$ and also $\mathcal{M}_2(\theta') = 0$. \mathcal{M}_2 is otherwise increasing, in a manner that ensures $[\mathcal{M}_1 - \mathcal{M}_2](\theta') = m_O(\theta')$. Then

$$R_{1,2}(+\theta) = [\mathcal{M}_1 - \mathcal{M}_2](+\theta) = m_O(+\theta).$$

Since $L_i[\mathcal{M}_i(-\theta)] = 0 - \mathcal{M}_i(-\theta)$ we have also

$$L_{1,2}(-\theta) = -[\mathcal{M}_1 - \mathcal{M}_2](-\theta) = -m_O(-\theta) = m_O(+\theta),$$

$$\hat{m}_O(\theta) = 2m_O(+\theta).$$

For the unreflected m_O^* , the right and left measures are reversed and $\hat{m}_O^*(\theta') = 2m_O^*(-\theta)$.

This completes the composite solutions for Eq.(11).

\hat{m} can also be obtained from a direct construction of \mathcal{M}_1 and \mathcal{M}_2 . When the maximum occurs for negative θ – as in m^* of Figure 4(a) – the composite is given by $\hat{m}(\theta) = m(-\theta) - m(+\theta)$; by definition of odd function this equals $2m_O(-\theta) = \hat{m}_O$.

A complete solution for an arbitrary even function requires also consideration of a function, m_{E° say, with $m_{E^\circ}(0) = m_{E^\circ}(\pm\infty)$. The simplest such function can be

obtained from the previous odd function by reflecting $m_O(-\theta)$, the negative half of m_O , while retaining the positive half. That is,

$$m_{E^\circ}(+\theta) = m_{E^\circ}(-\theta) = m_O(+\theta).$$

The construction for m_{E° differs from the previous monotone $m_E^*(+\theta)$. $\mathcal{M}_1[m_{E^\circ}(\theta')]$ is the same as in m_O , as is also $\mathcal{M}_2(+\theta)$, whence $R_{1,2}$ remains the same, equal to $m_{E^\circ}(+\theta)$. For left measures, even though the increasing and decreasing segments for $m_{E^\circ}(-\theta)$ are the reverse of $m_O(-\theta)$, we still have

$$L_{1,2}(-\theta) = -[\mathcal{M}_1 - \mathcal{M}_2](-\theta) = -m_{E^\circ}(-\theta),$$

Hence, as for m_E^* , we have $\hat{m}_{E^\circ} = 0$. Thus the composite distribution for any symmetric function is zero.

The question arises whether a symmetric function $m_E(\theta|y)$ with $m_E(0) = 0$, similar to m_{E° , can be realized (with varying y) as a translation-related composite FM. Using the “density subtended area” procedure with the varying θ interval $[-\theta+y, +\theta+y]$, one can readily verify that the symmetric RD density defined by $f(x) = 0$ for $-a < x < +a$ and otherwise non-zero symmetric, yields the following FM’s: For $y < a$, $m_E(\theta'|y) = 0$ for $|\theta'| < a$ (a modified m_{E°); for $y = a$, $m_E = m_{E^\circ}$; and for $y > a$, m_E is similar to m_E^* in Figure 4(b).

The previous analysis for m_O^* applies also to odd functions where the limiting values for plus infinity and minus infinity are not the same. (This case represents a non-monotone generalization of the ordinary application of Eq.(6) in obtaining the distribution of y .) The composite distribution for any odd function $m_O(\theta')$ is then also given by $2m_O(+\theta)$.

References

- [1] Cramér, H. (1946), *Mathematical Methods of Statistics*, Princeton University Press.

- [2] Fisher, R.A. (1930), "Inverse probability," *Proc. of the Cambridge Phil. Society*, 26, 528-535.
- [3] Fisher, R.A. (1956), *Statistical Methods and Scientific Inference*, Edinburgh: Oliver and Boyd.
- [4] Graves, L.M. (1946), *The Theory of Functions of Real Variables*, First Edition, New York, McGraw Hill.
- [5] Haaser, N.B. and Sullivan, J.A. (1971), *Real Analysis*, Van Nostrand.
- [6] Halmos, P.R. (1950), *Measure Theory*, New York, Van Nostrand.
- [7] Hannig, J. (2009), "On generalized fiducial inference," *Statistica Sinica*, 19, 491-544.
- [8] Lindley, D.V. (1958), "Fiducial distributions and Bayes' theorem," *J. of Royal Stat. Soc., Series B* 20, 102-107.
- [9] Pinkham, R.S. (1966), "On a Fiducial Example of C. Stein," *J. of Royal Stat. Soc., Series B* 28, 53-54.
- [10] Seidenfeld, T. (1992), "R.A. Fisher's fiducial argument and Bayes' theorem," *Stat. Sci.* 7, 358-368.
- [11] Stein, C. (1959), "An example of wide discrepancy between fiducial and confidence intervals," *Ann. Math. Stat.*, 30, 877-880.
- [12] Stigler, S.M. (1990), *The History of Statistics: The Measurement of Uncertainty before 1900*, Harvard University Press.
- [13] Tukey, J.W. (1957), "Some examples with fiducial relevance," *Ann. Math. Stat.*, 28, 687-695.

Acknowledgment

My thanks and appreciation go to Professor Refael Hassin. Rafi generously took upon himself various responsibilities, including computerizing the figures and converting many drafts, which used antiquated equation software, into error-free pdf files. Without his encouragement and patience, his numerous technical and non-technical suggestions, and his excellent advice to not wait until the concomitant applications

paper was completed, this present paper would probably not exist, now nor in the foreseeable future.